ITALIAN PHYSICAL SOCIETY
SOCIETÀ ITALIANA DI FISICA

Particle Beam Diagnostics and Control

Part 2: Transverse Phase Space

Gero Kube
DESY / MDI
gero.kube@desy.de

- Introduction
- Emittance Diagnostics
- Profile Monitors

Accelerator Key Parameters

light source: spectral brilliance

- measure for phase space density of photon flux

$$B = \frac{\text{Number of photons}}{[\text{sec}][\text{mm}^2][\text{mrad}^2][0.1\%\ \text{bandwidth}]}$$

- user requirement: high brightness

  → lot of monochromatic photons on sample

- connection to machine parameters

$$B \propto \frac{N_\gamma}{\sigma_x \sigma_{x'} \sigma_z \sigma_{z'}} \propto \frac{I}{\varepsilon_x \varepsilon_z}$$

- requirements

i) high beam current

- achieve high currents
- cope with high heat load (stability)

collider: luminosity L

- measure for the collider performance

$$\dot{N} = L \cdot \sigma$$

relativistic invariant proportionality factor between cross section σ (property of interaction) and number of interactions per second

- user requirement: high luminosity

  → lot of interactions in reaction channel

- connection to machine parameters

$$L \propto \frac{I_1 \cdot I_2}{\varepsilon}$$

for two identical beams with emittances $\varepsilon_x = \varepsilon_z = \varepsilon$

ii) small beam emittance

- achieve small emittance (task of lattice designer)
- preserve emittance (stability)
- measure small emittance

Transverse Phase Space

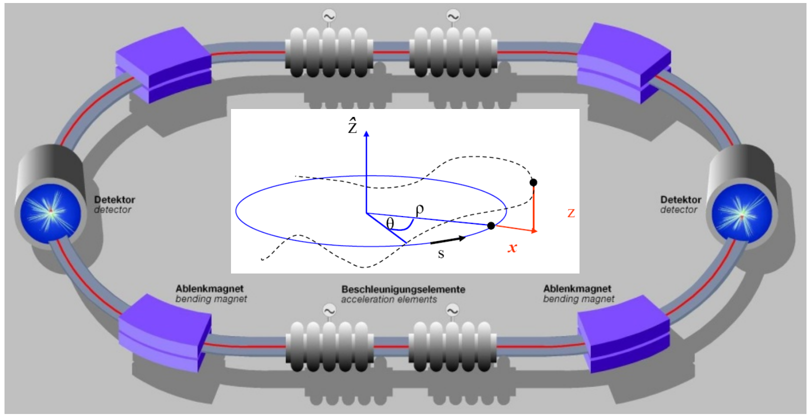

- **equation of motion**
  - Hill´s type differential equation

$$x''(s) + \left(\frac{1}{\rho^2(s)} - k(s) \right) \cdot x(s) = \frac{1}{\rho(s)} \Delta p / p$$

$$z''(s) + k(s) \cdot z(s) = 0 \qquad k = \frac{e}{p} \frac{\partial B_z}{\partial x}$$

- **emittance**
  - 6-dim. phase space volume
    → use areas of projection onto 3 orthogonal planes
  - evolves out of Hamilton formalsim, hence based on canonical coordinates
    → instead of phase space in (x, p_x) use (x, $x' = p_x / p_z$)
  - constant of motion (Liouville´s theorem)
    → area preserved
    → independent on location in accelerator

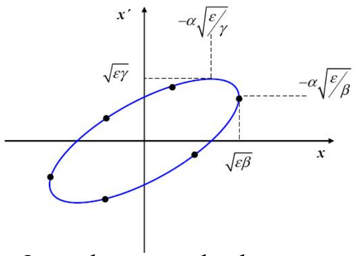

- **solution: quasi-periodic motion**

$$x(s) = \sqrt{\varepsilon \beta_x(s)} \cdot \cos(\Psi(s) + \Phi)$$

beam size

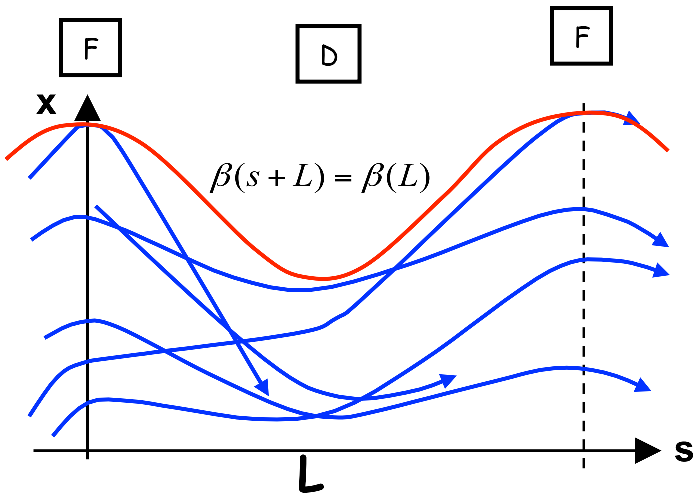

Transverse Emittance

- linear forces
  - any particle moves on an ellipse in phase space (x,x´)
  - ellipse rotates in magnets and shears between magnets

    → but area is preserved: **emittance**

    (<u>acceleration:</u> normalized emittance preserved)

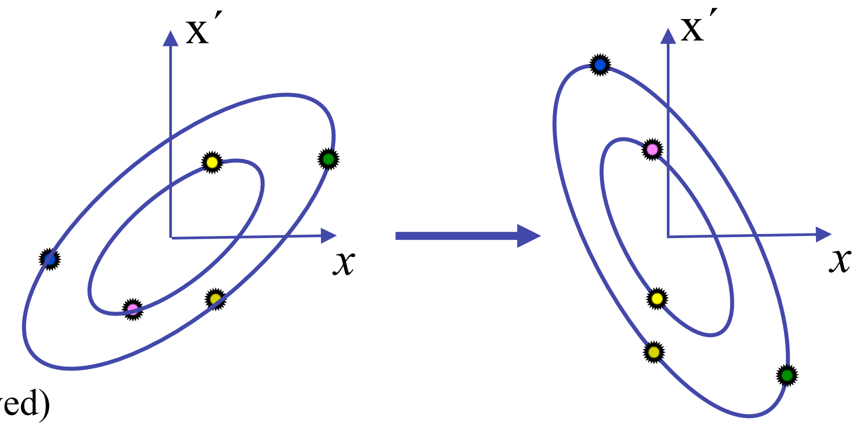

phase space evolution

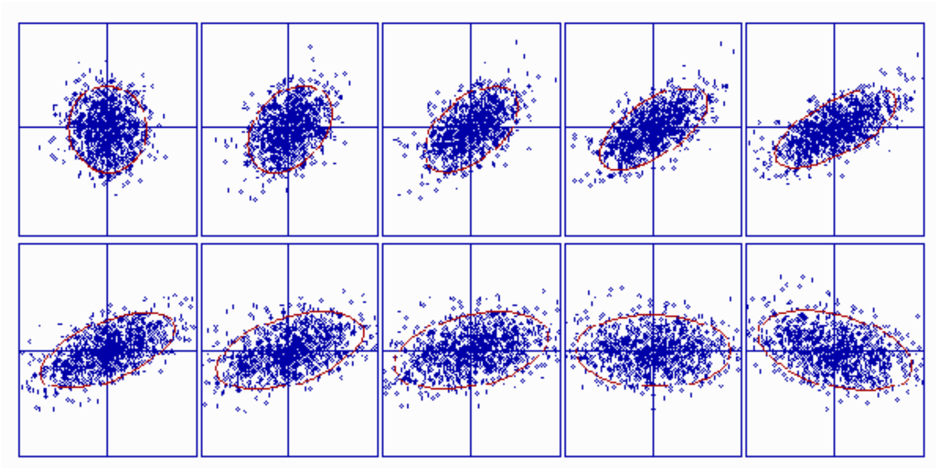

- general ellipse equation

$$\varepsilon = \gamma \cdot x^2 + 2\alpha \cdot x\,x' + \beta \cdot x'^2$$

- α, β, γ, ε: **Courant-Snyder** or **Twiss** parameters

  → **α, β, γ:** functions of location s in accelerator

  → **ε:** constant. Ellipse area = πε

- 4 Twiss parameters, only 2 of them are independent:

$$\gamma = \frac{1+\alpha^2}{\beta}$$

courtesy: C.R. Prior (Rutherford Lab)

Emittance and Beam Matrix

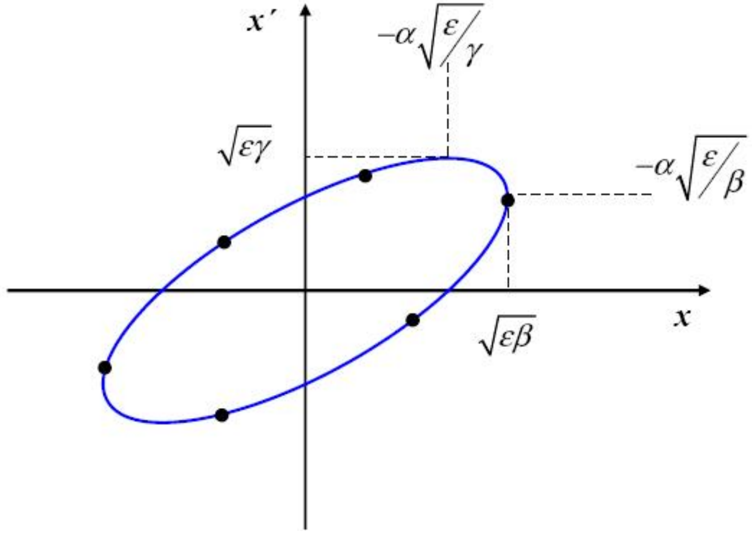

- via Twiss parameters

$$\varepsilon = \gamma x^2 + 2\alpha x x' + \beta x'^2$$

- statistical definition

P.M. Lapostolle, IEEE Trans. Nucl. Sci. NS-18, No.3 (1971) 1101

$$\varepsilon_{rms} = \sqrt{\langle x^2\rangle\langle x'^2\rangle - \langle xx'\rangle^2}$$

2nd moment of beam distribution ρ(x)

$$\langle x^2\rangle = \frac{\int_{-\infty}^{\infty} \mathrm{d}x\, x^2 \cdot \rho(x)}{\int_{-\infty}^{\infty} \mathrm{d}x\, \rho(x)}$$

- ε_{rms} is measure of spread in phase space
- root-mean-square (rms) of distribution

$$\sigma_x = \langle x^2\rangle^{1/2}$$

- ε_{rms} useful definition for non-linear beams

→ usually restriction to certain range

(c.f. 90% of particles instead of [-∞,+∞])

- beam matrix

$$\sigma = \begin{pmatrix} \sigma_{11} & \sigma_{12} \\ \sigma_{21} & \sigma_{22} \end{pmatrix} = \begin{pmatrix} \langle x^2\rangle & \langle xx'\rangle \\ \langle xx'\rangle & \langle x'^2\rangle \end{pmatrix} = \varepsilon \begin{pmatrix} \beta & -\alpha \\ -\alpha & \gamma \end{pmatrix}$$

$$\varepsilon = \sqrt{\det \sigma} = \sqrt{\sigma_{11}\cdot\sigma_{22} - \sigma_{12}^2}$$

- transformation of beam matrix

$$\sigma^1 = \boldsymbol{R}\sigma^0\boldsymbol{R}^T \qquad R = \begin{pmatrix} R_{11} & R_{12} \\ R_{21} & R_{22} \end{pmatrix}$$

Emittance Measurement: Principle

- emittance: projected area of transverse phase space volume
- not directly accessible for beam diagnostics

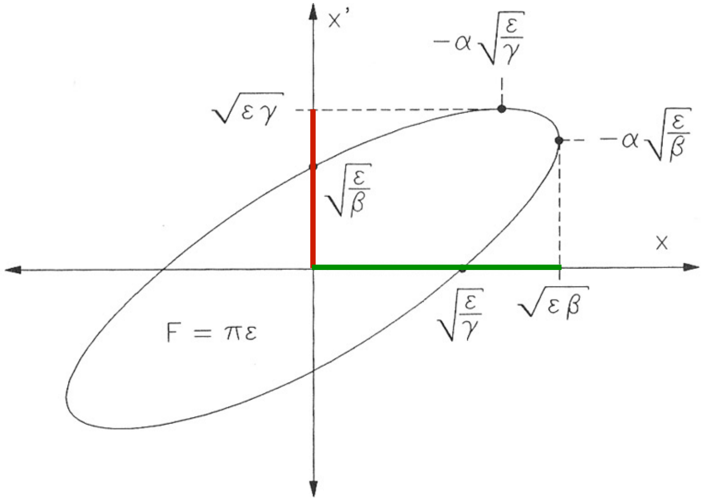

- measured quantity
  - beam size $\sqrt{\sigma_{11}} = \sqrt{\langle x^2 \rangle} = \sqrt{\varepsilon\beta}$
  - beam divergence $\sqrt{\sigma_{22}} = \sqrt{\langle x'^2 \rangle} = \sqrt{\varepsilon\gamma}$
  - divergence measurements seldom in use

    → restriction to profile measurements

- measurement schemes
  - beam matrix based measurements

    → determination of beam matrix elements: $\varepsilon = \sqrt{\det\sigma} = \sqrt{\sigma_{11}\cdot\sigma_{22} - \sigma_{12}^2}$
  - mapping of phase space

    → restrict to (infenitesimal) element in space coordinate, convert angles x‘ in position

Beam Matrix based Measurements

- starting point: beam matrix
$$\sigma = \begin{pmatrix} \sigma_{11} & \sigma_{12} \\ \sigma_{21} & \sigma_{22} \end{pmatrix} = \begin{pmatrix} \langle x^2 \rangle & \langle xx' \rangle \\ \langle xx' \rangle & \langle x'^2 \rangle \end{pmatrix} = \varepsilon \begin{pmatrix} \beta & -\alpha \\ -\alpha & \gamma \end{pmatrix}$$

- emittance determination
  - measurement of **3** matrix elements **σ_{11}, σ_{12}, σ_{22}**
  - **remember:** beam matrix σ depends on location, i.e. σ(s)

    → determination of matrix elements at same location required

$$\varepsilon = \sqrt{\det \sigma} = \sqrt{\sigma_{11} \cdot \sigma_{22} - \sigma_{12}^2}$$

- access to matrix elements
  - profile monitor determines only $\sqrt{\sigma_{11}}$
  - other matrix elements can be inferred from beam profiles taken under various transport conditions

    → knowledge of transport matrix R required

$$\sigma^b = R \cdot \sigma^a \cdot R^T \qquad R = \begin{pmatrix} R_{11} & R_{12} \\ R_{21} & R_{22} \end{pmatrix}$$

- measurement of at least 3 profiles for 3 matrix elements

$$\sigma_{11}^a$$
$$\sigma_{11}^b = R_{11}^2 \cdot \sigma_{11}^a + 2R_{11}R_{12} \cdot \sigma_{12}^a + R_{12}^2 \cdot \sigma_{22}^a$$
$$\sigma_{11}^c = \bar{R}_{11}^2 \cdot \sigma_{11}^a + 2\bar{R}_{11}\bar{R}_{12} \cdot \sigma_{12}^a + \bar{R}_{12}^2 \cdot \sigma_{22}^a$$

  - **measurement :** profiles $\sigma_{11}^a, \sigma_{11}^b, \sigma_{11}^c$
  - **known:** transport optics $R, \bar{R}$
  - **deduced:** matrix elements $\sigma_{11}^a, \sigma_{12}^a, \sigma_{22}^a$

  → more than 3 profile measurements favourable, data subjected to least-square analysis

Beam Matrix based Measurements

- „quadrupole scan“ method
  - use of variable quadrupole strengths

    → change quadrupole settings and measure beam size in profile monitor located downstream

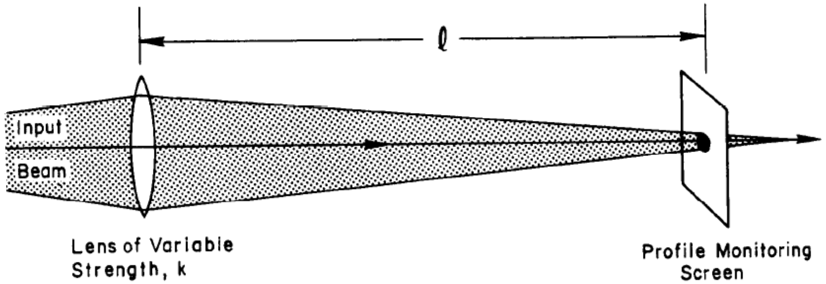

Q (f = 1/K) **S** (drift space)

- σ_{11} depends quadratically on quadrupole field strength

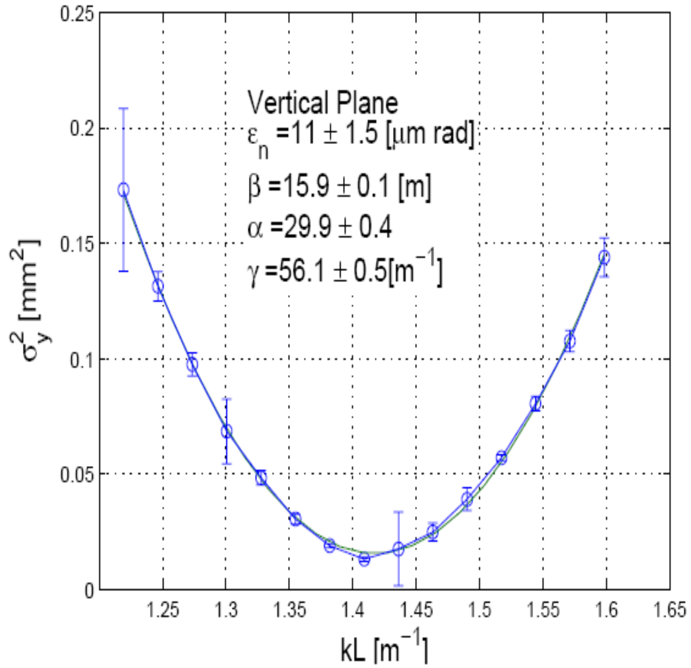

G. Penco et al., Proc. EPAC'08, Genoa (Italy), p.1236

quadrupole transfer matrix

$$Q = \begin{pmatrix} 1 & 0 \\ \pm 1/f & 1 \end{pmatrix}$$

drift space transfer matrix

$$S = \begin{pmatrix} 1 & l \\ 0 & 1 \end{pmatrix}$$

→ **R = SQ**

Beam Matrix based Measurements

- „multi profile monitor“ method
  - fixed particle beam optics
    - → measure beam sizes using multiple profile monitors at different locations
  - example:

    emittance measurement

    setup at FLASH injector

courtesy: K. Honkavaara (DESY)

Phase Space Mapping

- limitations for quadrupole scan / multi-screen method
  - successive variations in parameter space required (perturbative profile measurements)
    - → no single-shot capability
  - measuring principle relies on undisturbed phase space evolution (linear beam optics)
  - low-energy beams: often **space charge limited**
    - → reduce space charge influence by cutting out beamlet

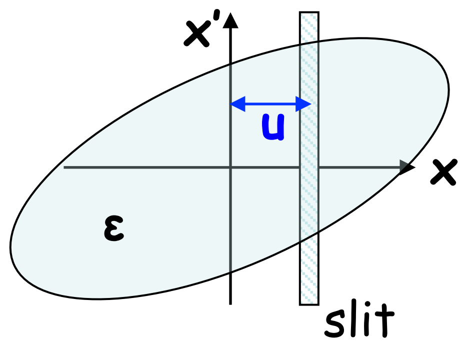

- „slit scanning" method
  - slit generates vertical slice (beamlet) in transverse phase space
    - → reduced space charge influence
  - convert angles into position through drift space L
    - → intensity at u, x´ in (x,x´)-space is mapped to position u+Lx´ defined by slit
  - profile measurement to reconstruct angular distribution
    - → scan with intensity monitor
    - → spatial resolving intensity measurement
  - successive scanning of slit to cover whole phase space

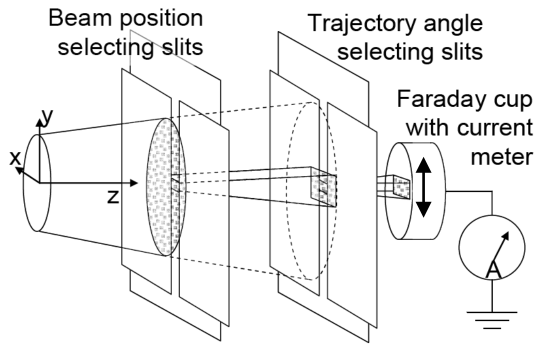

M.P.Stockli, Proc. BIW 2006, p.25

Phase Space Mapping

- comment: transformation of angular distribution to profile
  - moving through **drift space**
    → no change in angle
    (**horizonta**l move in phase space)
  - moving through **quadrupole**
    → no change in position
    (**vertica**l move in phase space)

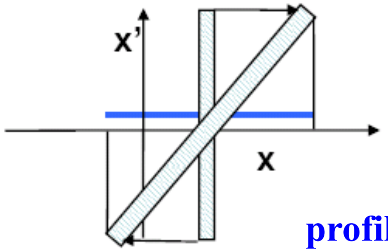

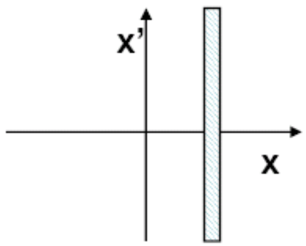

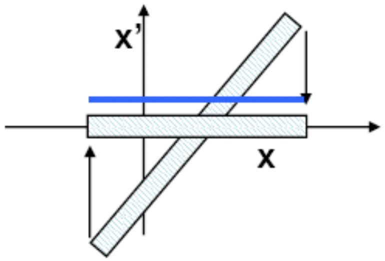

courtesy: U. Raich (CERN)

- multi-slit absorber
  - time consuming slit-scanning → multi-slit arrangement → 1-dim. single shot measurement

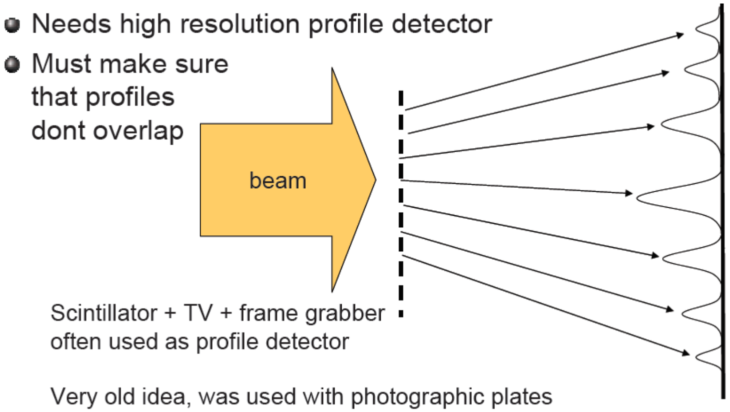

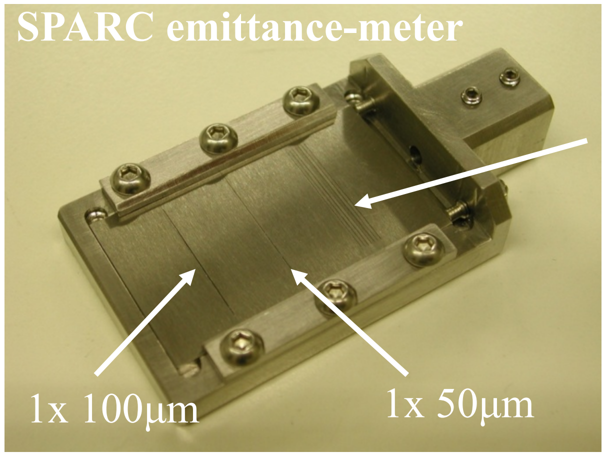

7x 50µm 500µm spaced

courtesy: A. Cianchi (Tor Vergata, Roma & INFN Frascati)

Phase Space Mapping

- emittance analysis

M. Zhang, *Emittance Formula for Slits and Pepper-pot Measurements*, FERMILAB-TM-1988

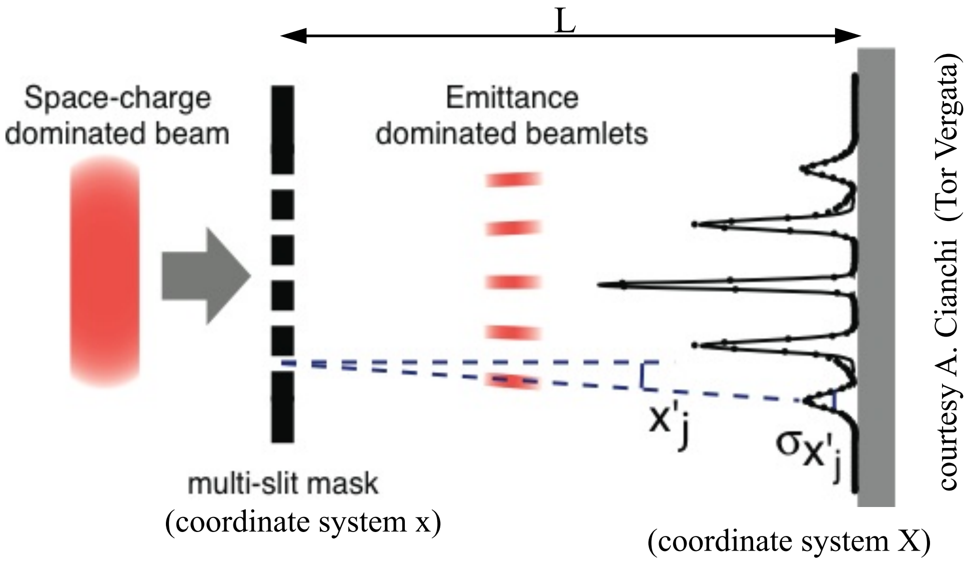

$$\varepsilon_{rms} = \sqrt{\langle x^2\rangle\langle x'^2\rangle - \langle xx'\rangle^2}$$

$$\langle x^2\rangle = \frac{1}{N}\sum_{j=1}^{p} n_j\left(x_{sj} - \bar{x}\right)^2$$

$$\langle x'^2\rangle = \frac{1}{N}\sum_{j=1}^{p} n_j\left[\sigma_{x'j}^2 + \left(\bar{x}'_j - \bar{x}'\right)^2\right]$$

$$\langle xx'\rangle = \frac{1}{N}\left(\sum_{j=1}^{p} n_j x_{sj}\bar{x}'_j - N\bar{x}\bar{x}'\right)$$

- p: total number of slits
- x_{sj}: j^th slit position
- n_j: number of particles passing thgough j^th slit
  → intensity weighting
- N: number of particles behind slits $N = \sum_{j=1}^{p} n_j$
- $\bar{x}$: mean position of all beamlets $\bar{x} = \frac{1}{N}\sum_{j=1}^{p} n_j x_{sj}$
- $\bar{x}'_j$: mean divergence of j^th beamlet
  $$\bar{x}'_j = \frac{\bar{X}_j - x_{sj}}{L} \quad \text{with} \quad \bar{X}_j = \frac{1}{n_j}\sum_{i=1}^{n_j} X_{ji}$$
- $\bar{x}'$: mean divergence of all beamlets
  $$\bar{x}' = \frac{1}{N}\sum_{i=1}^{p} n_j \bar{x}'_j$$
- $\sigma_{x'j}$: rms divergence of j^th beamlet
  $$\sigma_{x'j} = \frac{\sigma_j}{L} \quad \text{with} \quad \sigma_j^2 = \frac{1}{n_j}\sum_{i=1}^{n_j}\left(X_{ji} - \bar{X}_j\right)^2$$

Phase Space Mapping

- multi-slit absorber: practical considerations
  - grid of dense material (tungsten, tantalum) inserted in beam path
    - → split beam in several beamlets
    - → beam has to be fully absorbed i.e. works reliable only for low energetic beams
  - transverse position at which beamlets are created is known (position of grid)
    - → space coordinate
  - measurement of beamlet-size downstream (after drift space)
    - → access to beam divergence
  - beam size and beam divergence
    - → combined to emittance

example for space-charged dominated beam:

low-energy ion beam at GSI @ Darmstadt (Germany) behind source

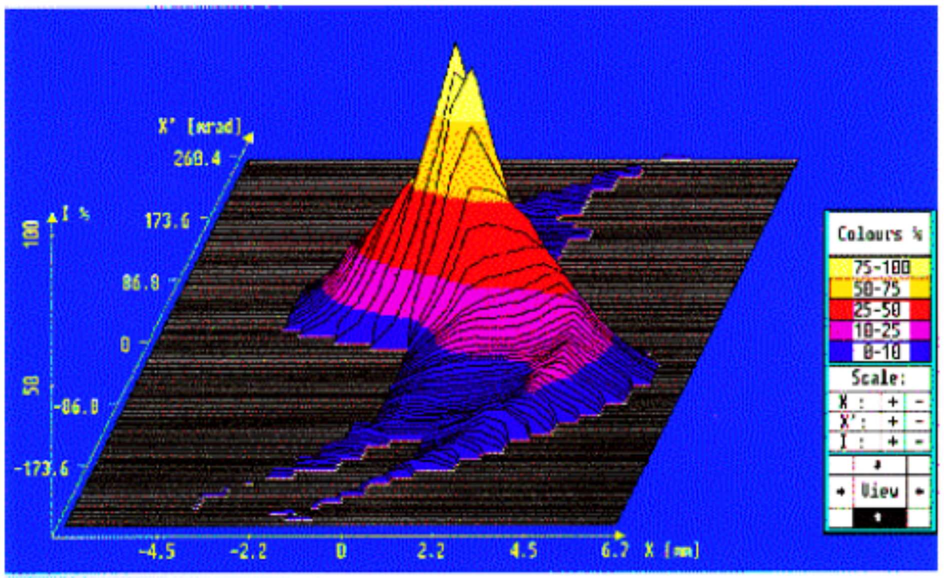

P. Forck, "Lecture Notes on Beam Instrumentation and Diagnostics", JUAS 2011

Phase Space Mapping

- pepper-pot: 2-dim. extension
  - matrix of holes in absorber plate
    - → single-shot capability for both planes
    - → investigation of shot-to-shot fluctuations
  - destructive method:

    tiny fraction of beam (ca. 1%) passes holes
    - → heat load in absorber has to be considered
    - → requires very sensitive detection system
  - also in use at Laser Plasma Accelerators

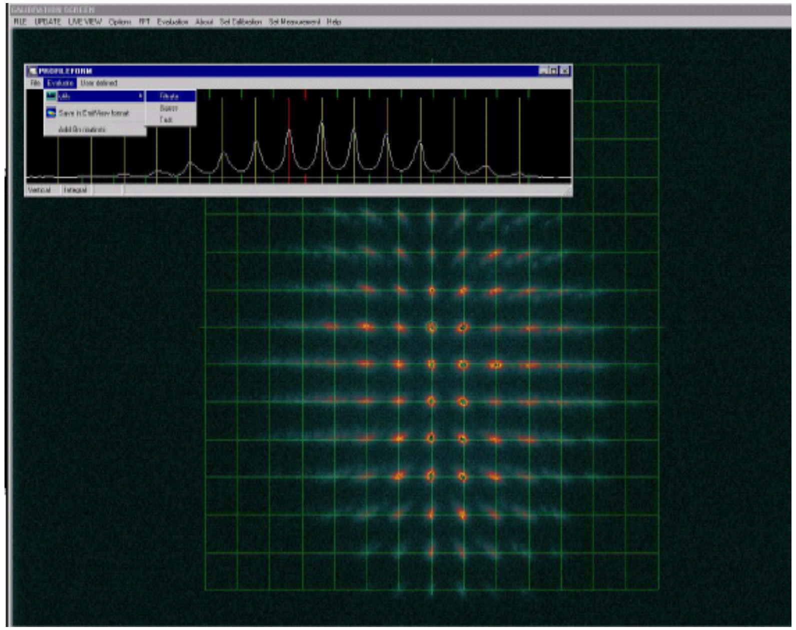

courtesy: P. Forck (GSI)

- useful references
  - M. Zhang, *Emittance Formula for Slits and Pepper-pot Measurements*, FERMILAB-TM-1988
  - S. Jolly et al., *Data Acquisition and Error Analysis for Pepperpot Emittance Measurements*, Proc. DIPAC'09, Basel, WEOA03

- limitations of slit / pepper-pot systems
  - best suited for low energy beams (≤ 100MeV)

    high energetic electron beam requires very thick absorber material → diffraction inside slit/hole
  - pepper-pot for 508 MeV electrons: N.Delerue et al., Proc. PAC'09, Vancouver (Canada), 2009, p.3597

Emittance Diagnostics: Comments

- comparison of different methods

	high energy	high space charge forces	large energy spread	single shot capability
slit / pepper-pot	-	+	+	+
quadrupole scan	+	-	- (chromatic effects)	-
multi-screen	+	-	+	-

according to H. Braun, "Emittance Diagnostics", CAS on Beam Diagnostics, Dourdan 2008

- emittance diagnostics in Linacs: non-parasitic and destructive measurements

- emittance diagnostics in circular accelerators
  - circular accelerator: periodic with circumference
    → Twiss parameters α(s), β(s), γ(s) uniquely defined at each location in ring
  - measurement at one location in ring sufficient to determine ε
    → measured quantity: beam profile / angular distribution

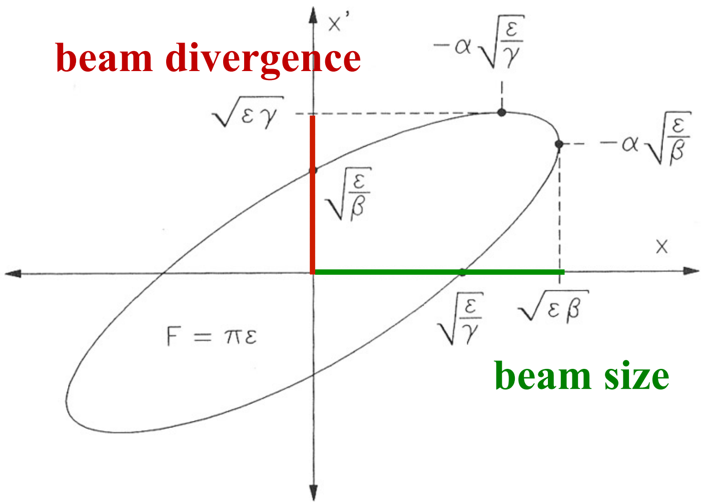

Slice Emittance

- commment: emittance at FELs
  - electrons slip back in phase with respect to photons by l_r each undulator period
  - FEL integrates over slippage length → **slice emittance** of importance

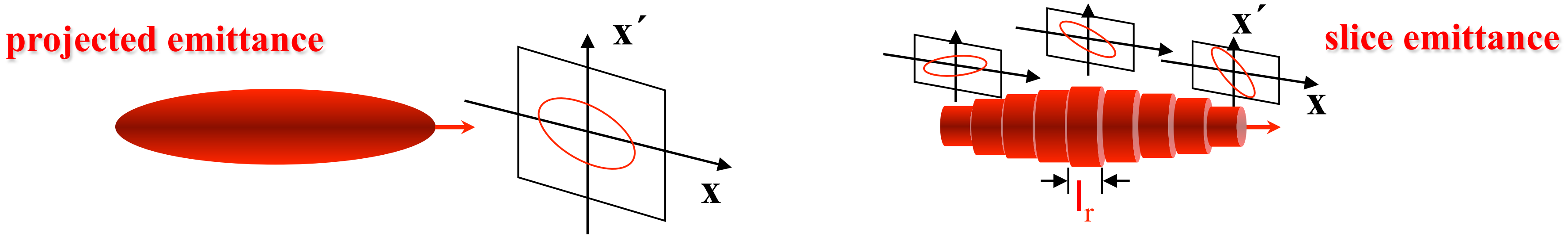

- measurement with transverse deflecting cavity

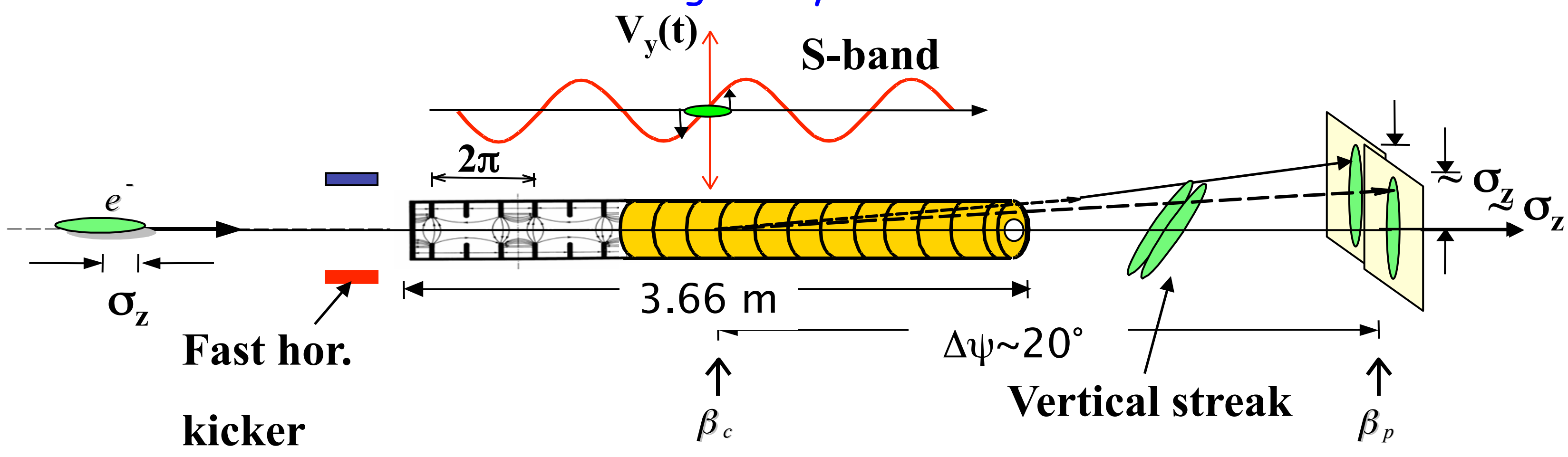

→ **discussion in 3rd lecture together with bunch length diagnostics**

Profile Measurements

- emittance diagnostics
  - underlying principle is profile measurement
  - profile contains information about angular/spatial distribution
- profile monitor: principles
  - consider beam with (for simplification 1-dim.) spatial distribution $\rho(x)$
  - generate secondary signal $\Sigma(x)$ with intensity proportional to $\rho(x)$
  - $\Sigma(x)$ is generated via

→ interaction of beam with matter	**wire scanner, scintillation screen,** residual gas monitor , secondary electron emission (SEM)…
→ interaction of beam with photons	laser wire scanner, …
→ separating particle beam electromegnetic field	synchrotron radiation, **OTR, ODR**, …

  - Σ can be flux of

→ charged particles	secondary electrons, …
→ electromagnetic radiation	visible light, γ-rays …

  - spatial resolution for detection of $\Sigma(x)$

→ scanning of conversion target or/and detector	wire, …
→ spatial resolving detector	optical detectors (CCD or CMOS sensors) , …

Wire Scanner

- advantages
  - direct and reliable measurement
  - resolution down to 1μm achieveable
  - minimum inivasive method

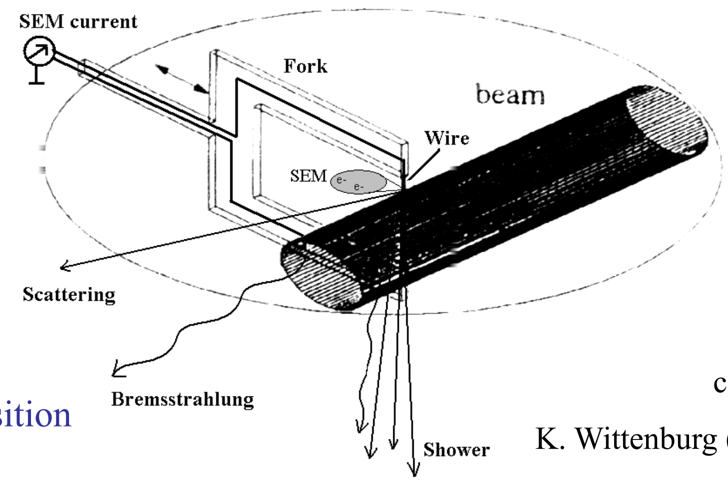

courtesy:
K. Wittenburg (DESY)

- operation principle
  - scanning of thin wire across the beam
  - detection of beam-wire interaction as function of wire position

- wire and mechanics
  - material: C, W, Be, …
  - wire size: down to few μm → limits resolution
  - fast wire movement (5-20 m/sec) for intense & high brilliant beams
    - → minimize emittance blow-up (circular hadron accelerators)
    - → reduce heat-load on wire: high melting temperature & low Z material
  - high speed movement
    - → rotationary wire movement : limited resolution down to 10-100 μm
    - → linear movement: speed limited by vacuum bellow stress properties
  - high precision encoder for position readout

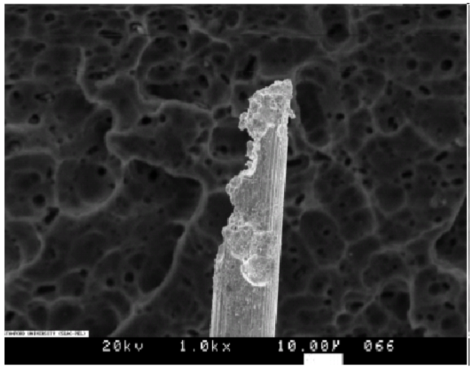

FIGURE 3. Failed 15 μm diameter tungsten wire showing the rough surface resulting from many discharges.

Wire Scanner

- **signal detection**
  - measure scattered beam particles and/or bremsstrahlung outside vacuum chamber
    - → fast scintillation counter (able to resolve single bunches)
    - → signal can depend on wire scanner location: Monte Carlo studies recommended
  - secondary electron emission in wire
    - → often used at low energy beams:
      - scattered particles cannot penetrate vacuum chamber
      - intensity of bremsstrahlung to low
    - → if wire temperature exceeds thermionic threshold: thermal electrons superimpose SEM signal

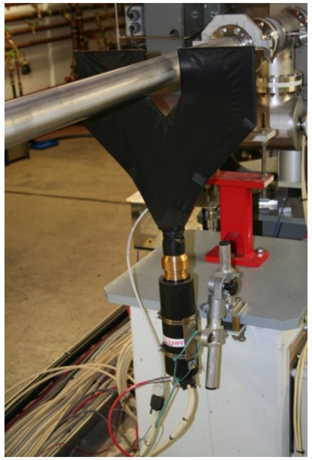

- **comments**
  - wire scanner measures projected beam profiles
    - → typically one scanner for each transverse plane required
  - option: wire scanner for both projections
    - → scanning under 45° geometry
  - information of x-y coupling
    - → installation of 3rd wire

      (bi-Gaussian with tilt: σ_x , σ_y , θ → requires 3 d.o.f.)

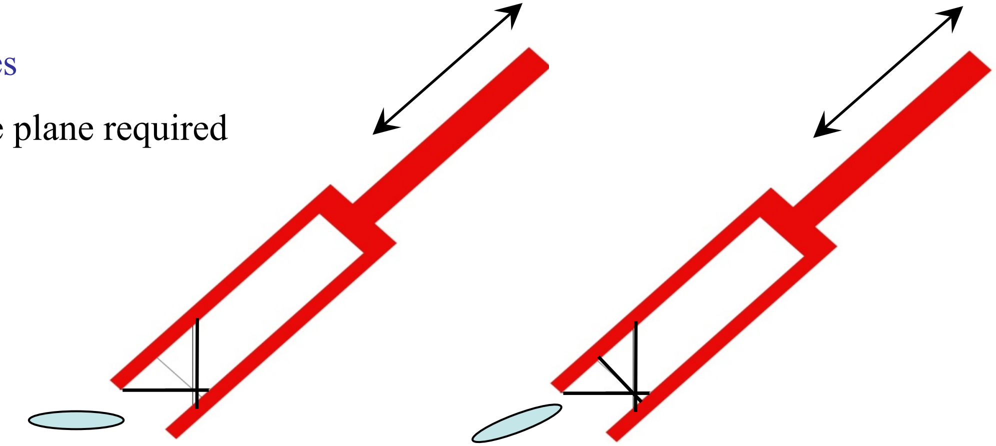

Wire Scanner for XFEL

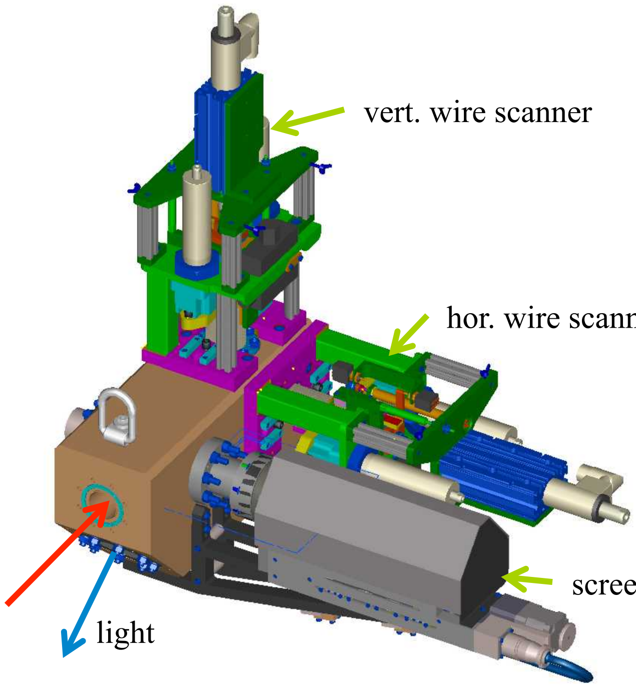

- wire scanners in combination with screen monitors
- scan speed 1m/sec
- design based on commercial linear motor
- drive and unit can be separated
  - → ease of maintenance
  - → flexibility of wire scanner distribution (COTR)

- wires and fork
  - → 3 wires for fast scan (W, 10-30 μm)
  - → 2 diagonal wires for optional coupling studies

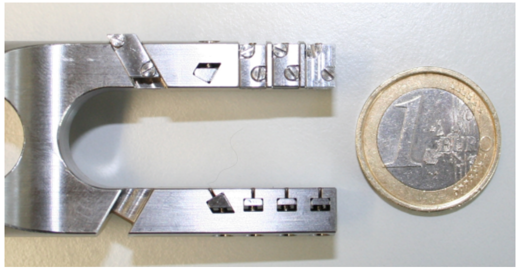

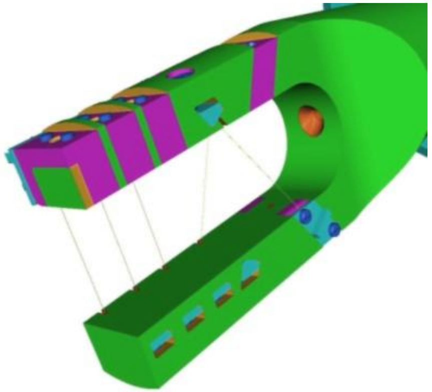

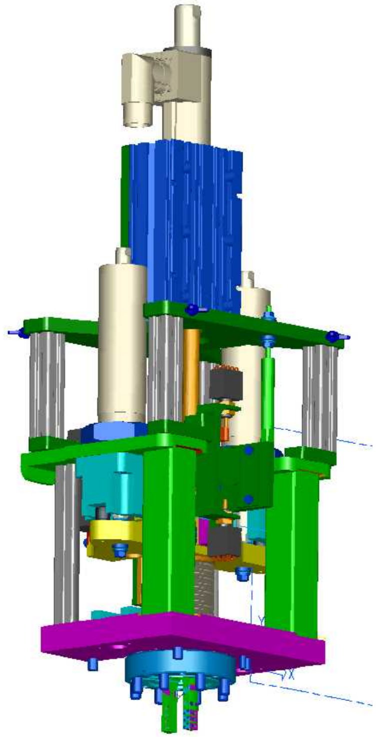

Harps

- profile diagnostics for hadron linacs
  - beam profiles in the order $\geq$ mm
  - instead of moving wire
    - → grid of wires: harp
    - → wire spacing down to a few hundreds of μm
  - measurement of SEM current

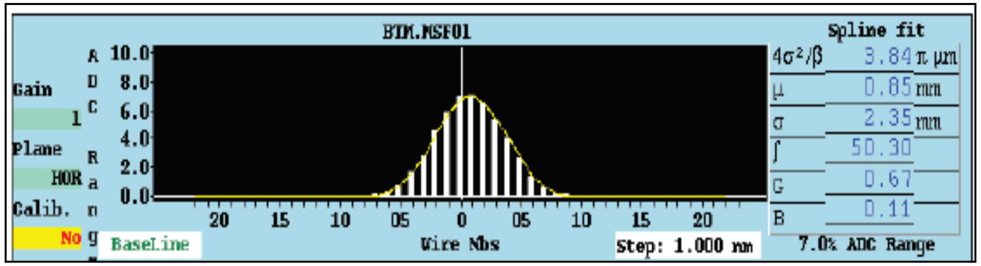

courtesy: U. Raich (CERN)

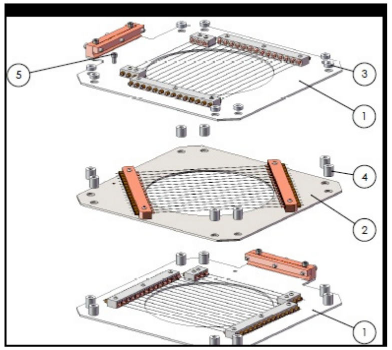

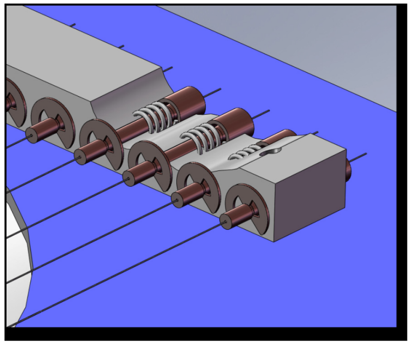

J. Douglas et. al, LANSCE Harp Upgrade , Proc. BIW2010, p.132

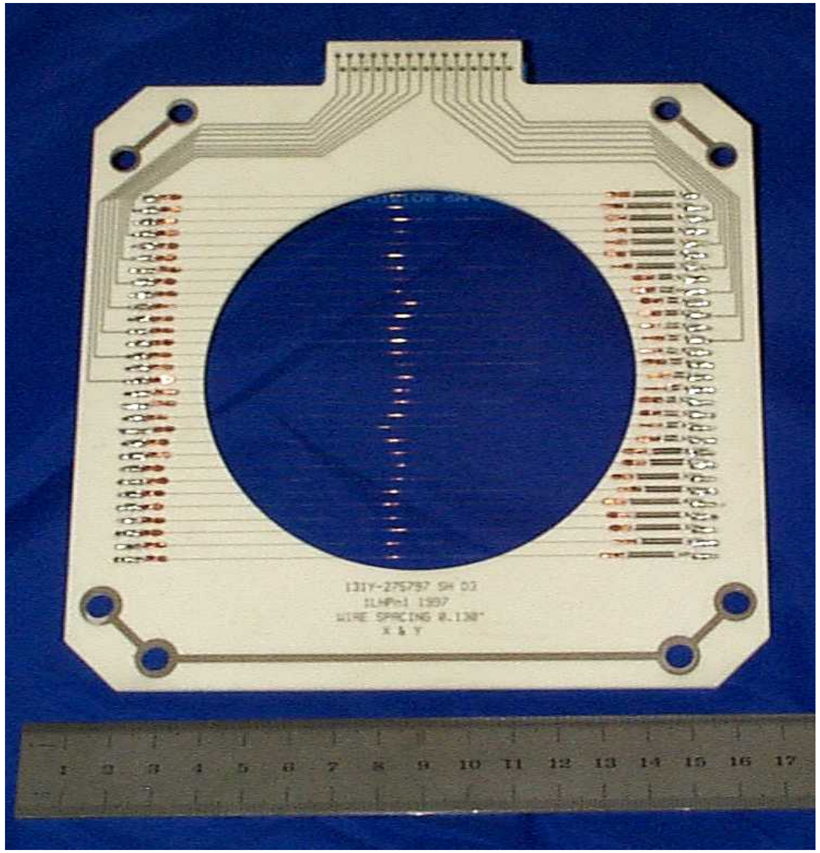

Harps in high radiation environments

11th ICFA International Mini-Workshop on Diagnostics for High-Intensity Hadron Machines, 2002, by Mike Plum

Laser Wire Scanner

- advantages
  - in principle resolution down to 1μm (and better?) achievable
  - non-invasive profile measurement
- principle
  - photons from Q-switched high power Nd:YAG laser collide with beam
    - → generation of forward Compton-scattered γ´s
  - transverse scanning of laser beam across electron beam
    - → γ intensity as function of laser poition: beam profile

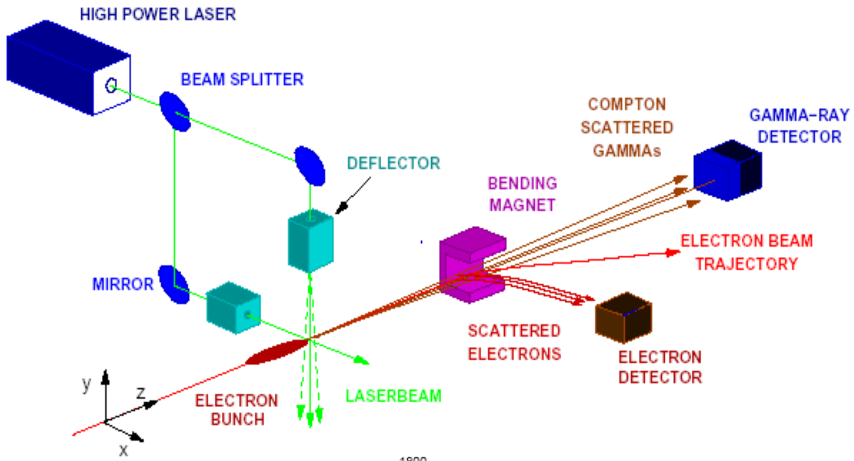

- device for reliable daily operation (?)
  - two test set-ups
    - → PETRA III @ DESY
    - → ATF2 @ KEK
  - PETRA experience
    - → so far expert system

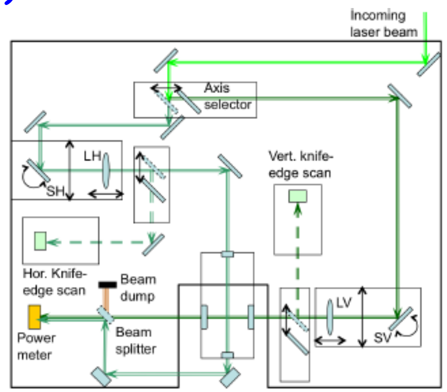

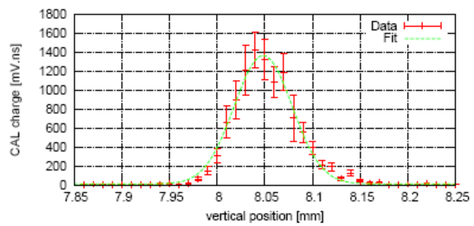

Figure 6: Vertical scan ($\sigma_y = 30.38 \pm 1.43\ \mu m$).

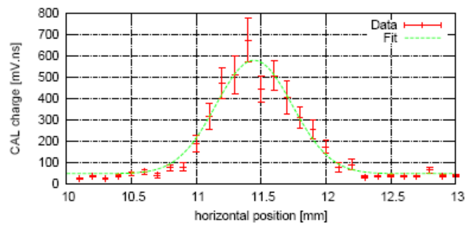

Figure 7: Horizontal scan ($\sigma_x = 293.6 \pm 18.1\ \mu m$).

T. Aumeyr et. al, Proc. IPAC'10, Kyoto (Japan), 2010 p.1137

Optical Profile Diagnostics

- taking advantage of the huge market for commercial available sensors
  - nowadays: high quality of optical light sensors for reasonable price
    - → small pixel size: high spatial resolution
    - → good linearity
    - → high dynamic range
  - optical beam diagnostics
    - → change from pure „visualization“ to high resolution measurements

- available light sensors
  - 1-D sensors
    - → photo diode array, line scan camera, segmented photomultiplier, …
    - → can be fast, up to hundreds of MHz

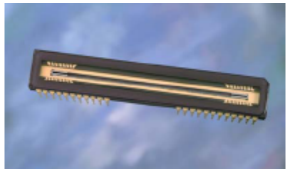

  - 2-D sensors
    - → area scan CCD & CMOS sensors, segmented photomultiplier, …
    - → usually slow (≈ 50 Hz), possible up to 100 kHz

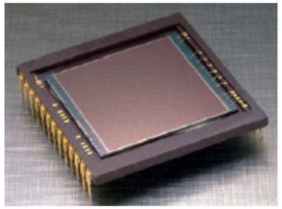

2-D sensors preferable because 2-D image contains whole spatial information

Profile Monitor Considerations

- **point of interest: monitor resolution**
  - consider single charged particle
  - calculate „point spread function“ (PSF) in image plane
  - convolute beam profile with PSF

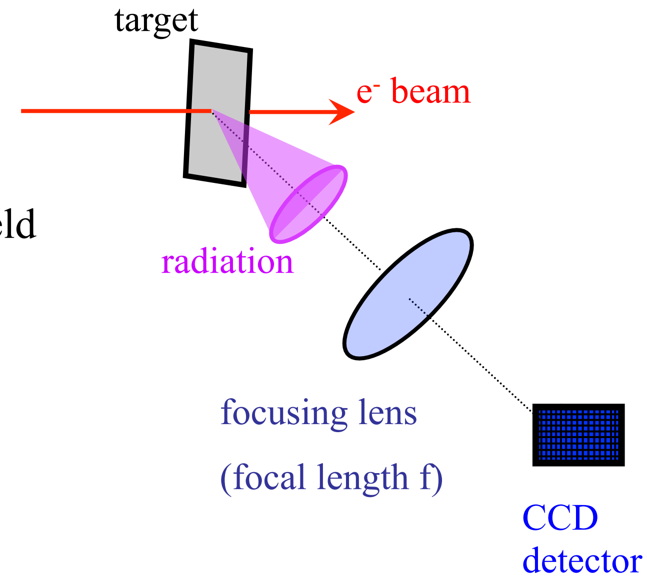

- **tasks**
  - radiation generation
    - ⟹ electromagnetic field distribution of radiation field
  - radiation propagation
    - ⟹ aperture limitations
  - focusing optics (lens)
    - ⟹ thin lens approximation
  - measurement of spatial intensity distribution
    - ⟹ PSF on CCD detector

Optical Propagation

- ...in frame of scalar diffraction theory

  - source plane to lens entrance

$$E^{l_{entr}}_{x_l,y_l}(\vec{r}_l,\omega) = -i\frac{e^{ika}}{\lambda a}\cdot e^{i\frac{k}{2a}\left(x_l^2+y_l^2\right)}\int\int_{source} dx_s dy_s\, E^{s}_{x_s,y_s}(\vec{r}_s,\omega)\cdot e^{i\frac{k}{2a}\left(x_s^2+y_s^2\right)}\cdot e^{-ik\frac{x_s x_l + y_s y_l}{a}}$$

  - lens input to lens output (thin lens approximation)

$$E^{l_{ext}}_{x_l,y_l}(\vec{r}_l,\omega) = E^{l_{entr}}_{x_l,y_l}(\vec{r}_l,\omega)\cdot e^{-i\frac{k}{2f}\left(x_l^2+y_l^2\right)}$$

with $\frac{1}{f} = \frac{1}{a} + \frac{1}{b}$

  - lens output to image plane (CCD detector)

$$E^{i}_{x_i,y_i}(\vec{r}_i,\omega) = -i\frac{e^{ikb}}{\lambda b}\cdot e^{i\frac{k}{2b}\left(x_i^2+y_i^2\right)}\int\int_{lens} dx_l\, dy_l\, E^{l_{ext}}_{x_l,y_l}(\vec{r}_l,\omega)\cdot e^{i\frac{k}{2b}\left(x_l^2+y_l^2\right)}\cdot e^{-ik\frac{x_l x_i + y_l y_i}{b}}$$

- measured quantity

  - spatial intensity distribution

$$\frac{\mathrm{d}^2 W}{\mathrm{d}\omega\,\mathrm{d}\Omega} = \frac{\mathrm{c}}{4\pi^2}\left(\left|\vec{E}^{i}_{x_i}(\vec{r}_i,\omega)\right|^2 + \left|\vec{E}^{i}_{y_i}(\vec{r}_i,\omega)\right|^2\right)$$

Radiation Generation: Considerations

- radiation generation via particle interaction with matter
  - luminescent screen monitors

- radiation generation via particle electromagnetic field
  - particle electromagnetic field

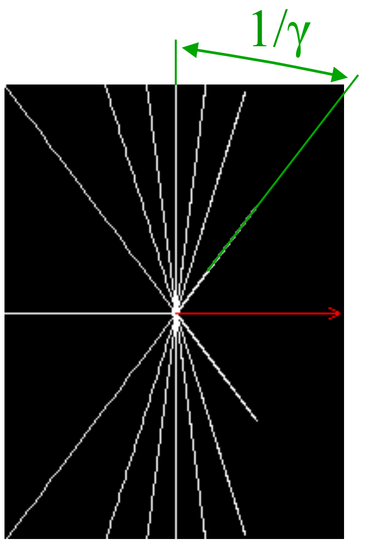

electric field lines
in LAB frame

  - relativistic contraction characterized by Lorentz factor

$$\gamma = E / m_0 c^2$$

E : total energy

$m_0 c^2$: rest mass energy

proton: $m_p c^2 = 938.272$ MeV

electron: $m_e c^2 = 0.511$ MeV

$\gamma \rightarrow \infty$: plane wave

- $mc^2 = 0$ MeV : light $\rightarrow$ „real photon“
- ultra relativistic energies : idealization $\rightarrow$ „virtual photon“

Separation of Particle Field

- electromagnetic field bound to particle
  observation in far field (large distances) } separate field from particle

- separation mechanisms
  - bending of particle via magnetic field

    synchrotron radiation

    ⟹ circular accelerators

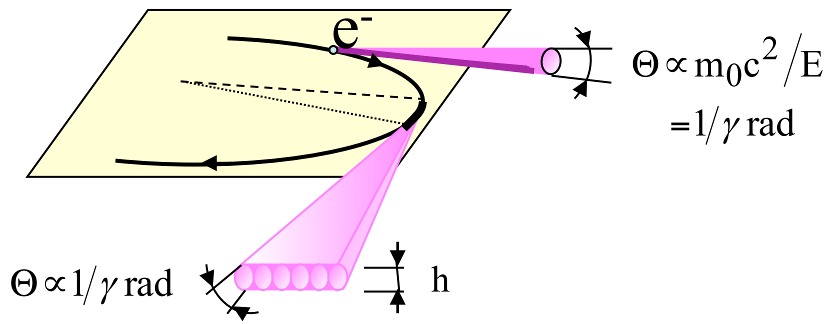

linear accelerators: no particle bending ???

  - diffraction of particle electromagnetic field via material structures

    exploit analogy between real/virtual photons:

    - light reflection/refraction at surface ↔ backward/forward transition radiation (TR)
    - light diffraction at edges ↔ diffraction radiation (DR)
    - light diffraction at grating ↔ Smith-Purcell radiation
    - light (X-ray) diffraction in crystal ↔ parametric X-ray radiation (PXR) …

Optical Transition Radiation

- transition radiation: electromagnetic radiation emitted when a charged particle crosses boundary between two media with different optical properties
- visible part: Optical Transition Radiation (OTR)
- beam diagnostics: backward OTR (reflection of virtual photons)
  typical setup: image beam profile with optical system
  → beam image and measurements of beam shape and size
- advantage: fast single shot measurement, linear response (neglect coherence !)
- disadvantage: high charge densities may destroy radiator, limitation on bunch number

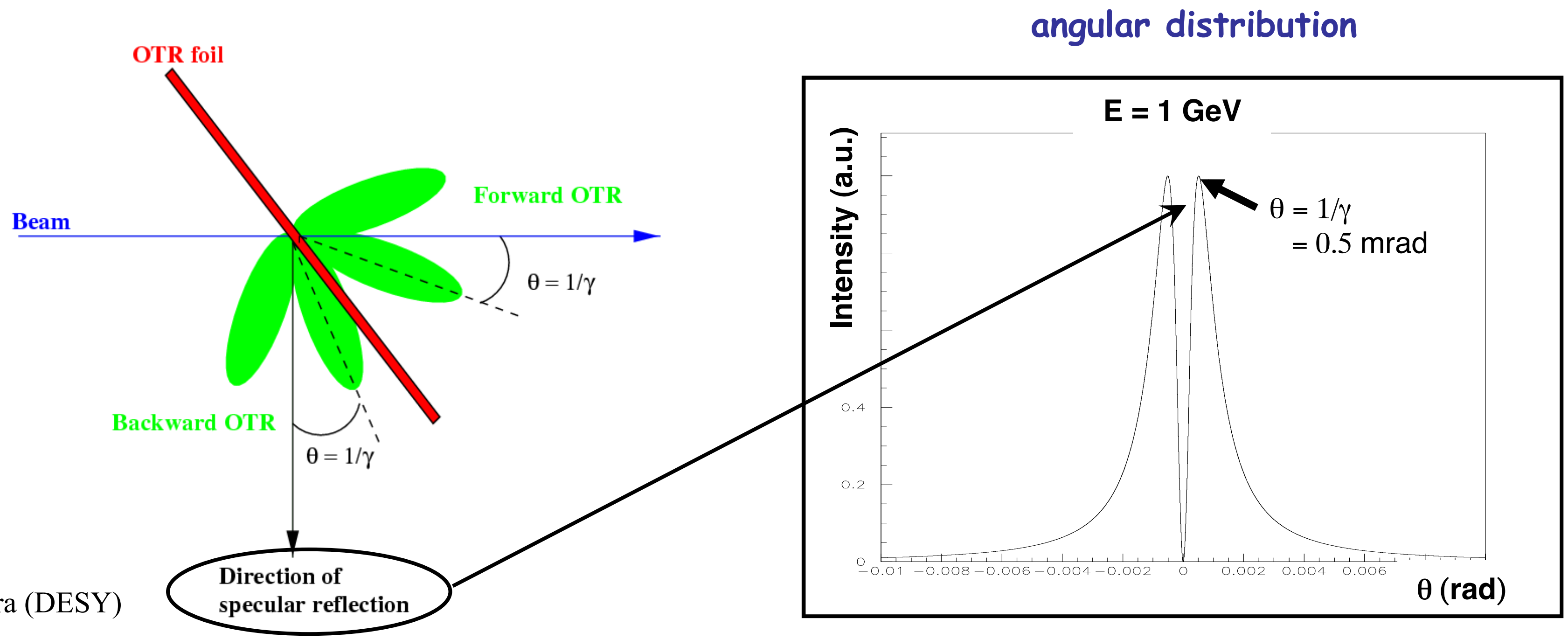

courtesy:
K. Honkavaara (DESY)

OTR Monitor Resolution

- calculation of point spread function in image plane

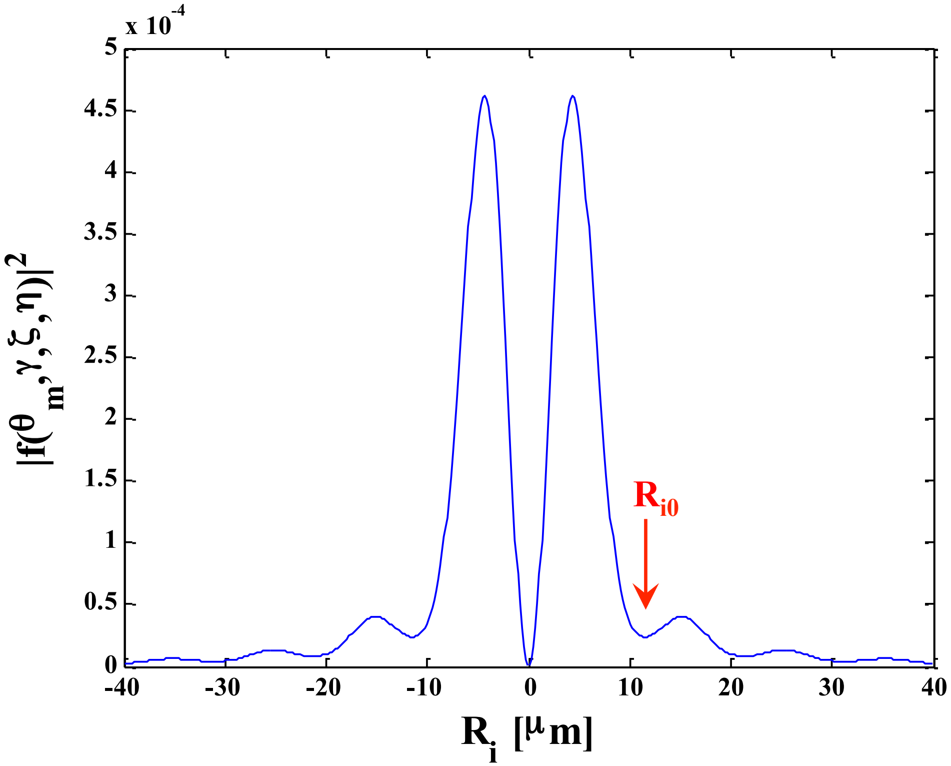

G. Kube, TESLA-FEL Report 2008-01

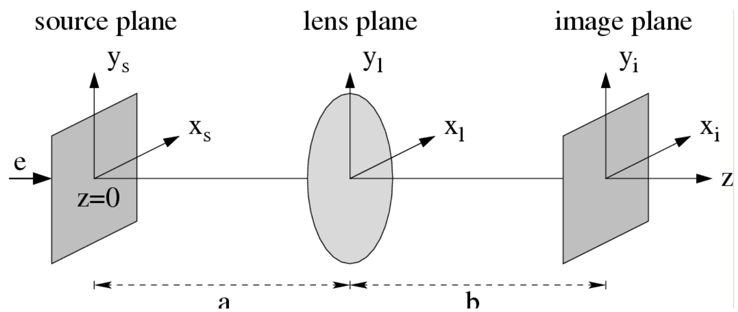

- parameters of calculation

E = 1 GeV
λ = 500 nm
f = 250 mm
a = b = 500 mm (1:1 imaging)
lens-Ø = 50.8 mm

- OTR resolution
  - resolution definition according to classical optics:

⟹ first minimum of PSF (→ diameter of Airy disk)

$$R_{i0} \approx 1.12 \frac{M\lambda}{\theta_m}$$

M: magnification
θ_m: lens acceptance angle

OTR Monitors at FLASH

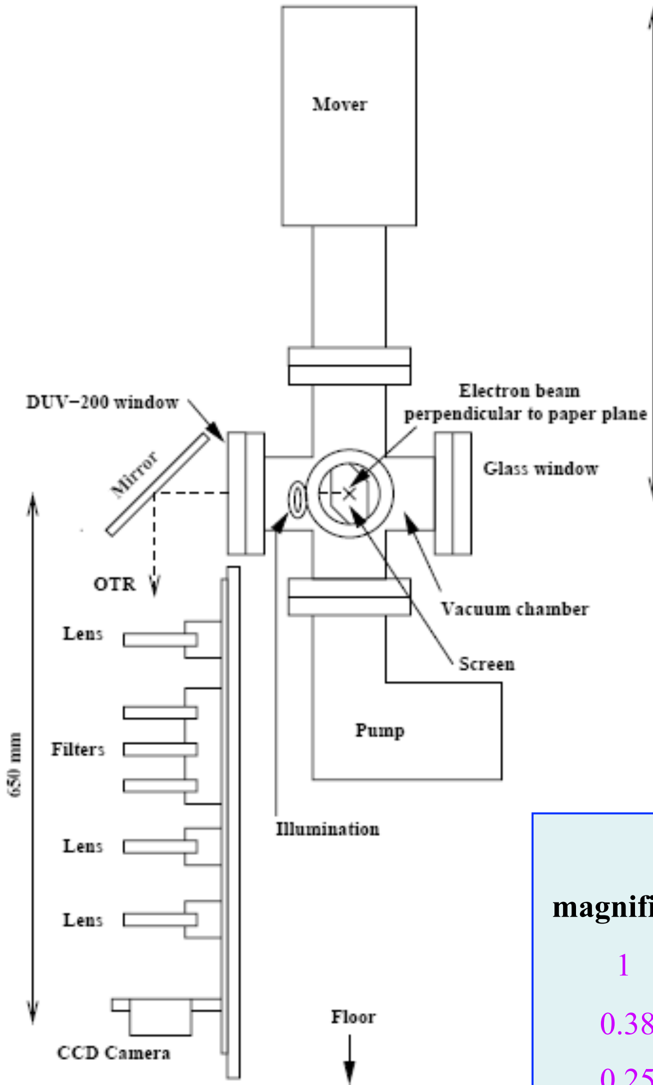

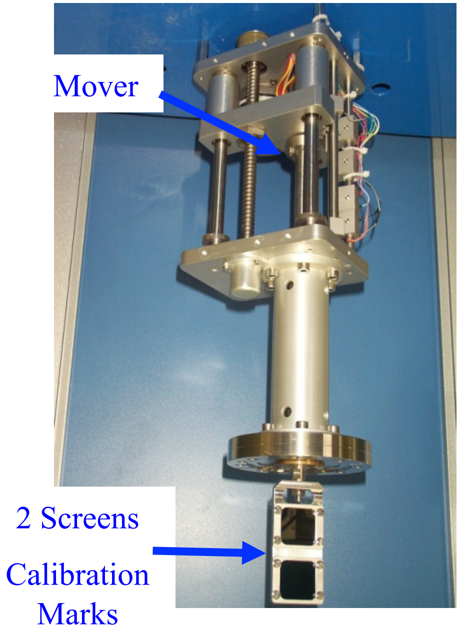

K. Honkavaara et al.,
Proc. PAC 2003, p.2476

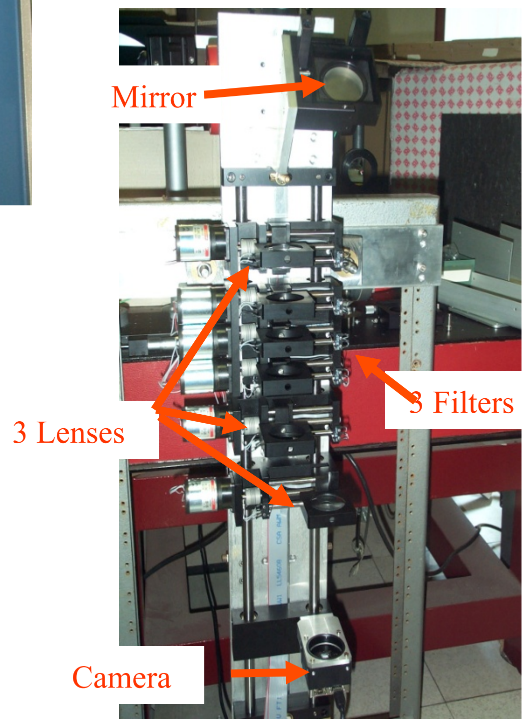

optical system

magnification	f / mm	a / mm	b / mm
1	250	500	500
0.382	200	724	276
0.25	160	800	200

Example of Beam Images (matched)

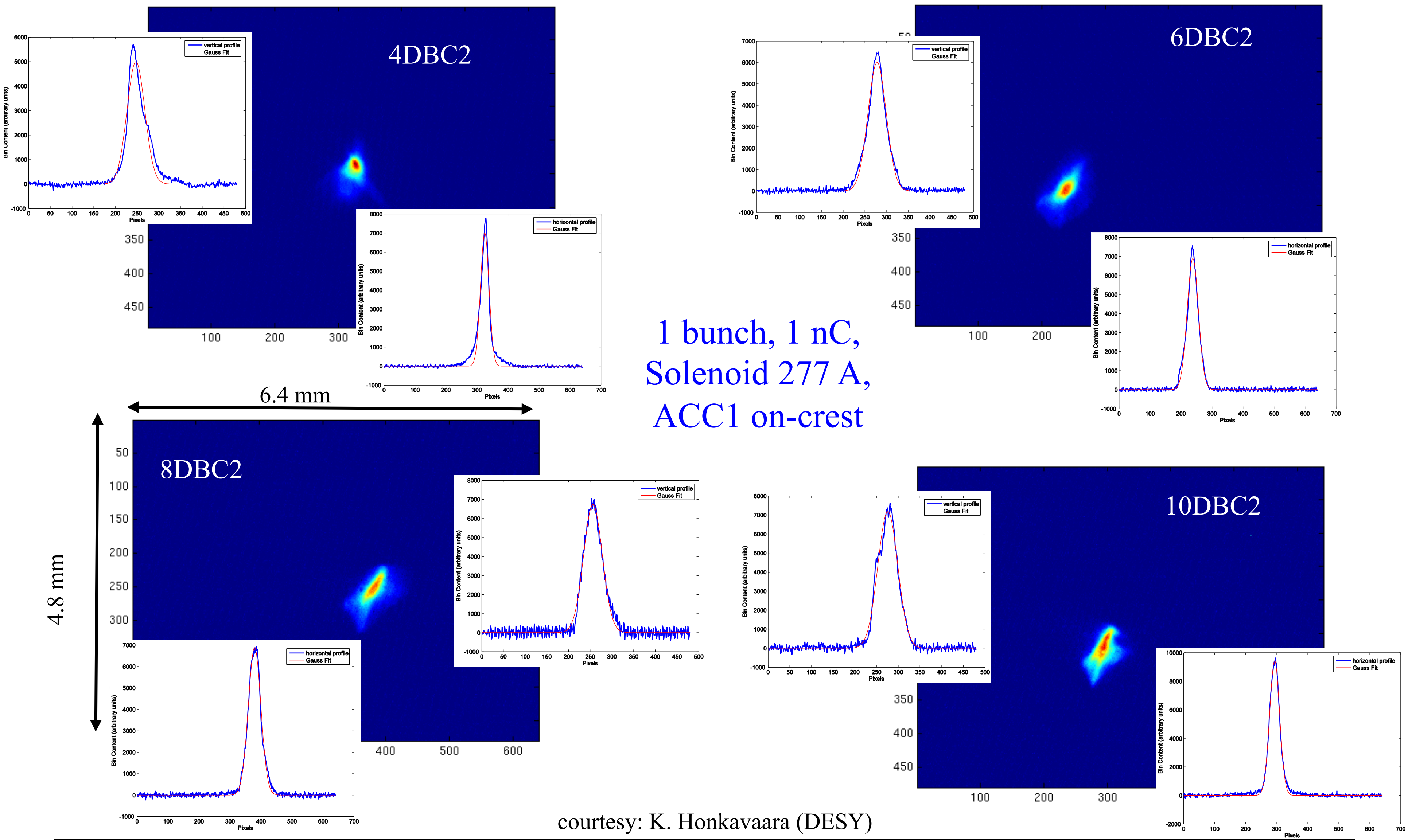

1 bunch, 1 nC,
Solenoid 277 A,
ACC1 on-crest

courtesy: K. Honkavaara (DESY)

XFEL OTR Monitors

- monitor setup

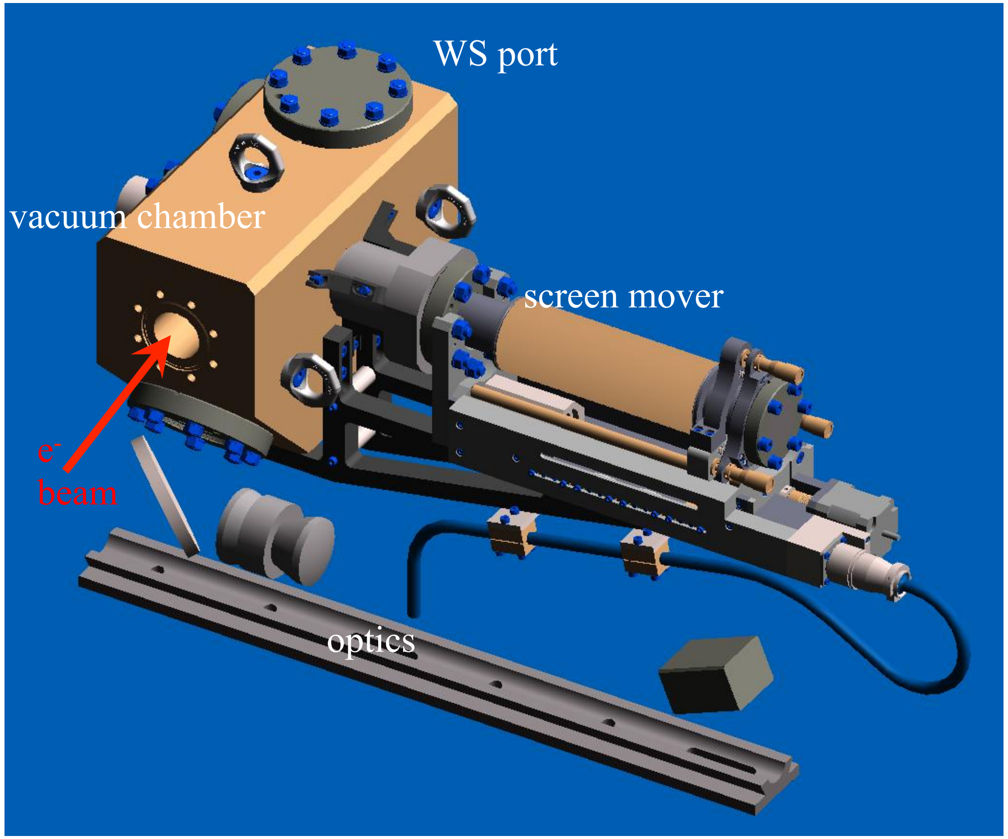

courtesy: Ch. Wiebers, D. Nölle (DESY)

- optics: **Scheimpflug** principle

from large format photography

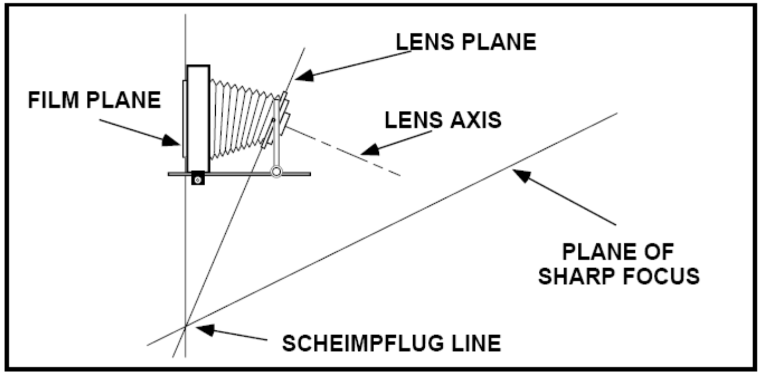

sharp image of an entire plane, if
- lens
- image
- object plane

cut in a single line

picture by Linhof

Optical Diffraction Radiation (ODR)

- problem OTR: screen degradation/damage

  → limited to only few bunch operation, no permanent observation

- ODR: excellent candidate to measure beam parameters parasitically

  - DR generation via interaction between the EM fields of the moving charge and the conducting screen

    → diffraction of "virtual photons"

  - extension of EM field of a relativistic particle is flat circle

    → radius $\lambda\beta\gamma/2\pi$

  - radiation intensity scales proportional to $|E|^2$:

$$I \propto e^{-a/h_{int}} \quad \text{with } h_{int} = \frac{\lambda\beta\gamma}{4\pi}$$

  - dependency on impact parameter h_{int}:

$$a \gg h_{int} : \text{no radiation}$$
$$a \cong h_{int} : \text{DR}$$
$$a \ll h_{int} : \text{TR}$$

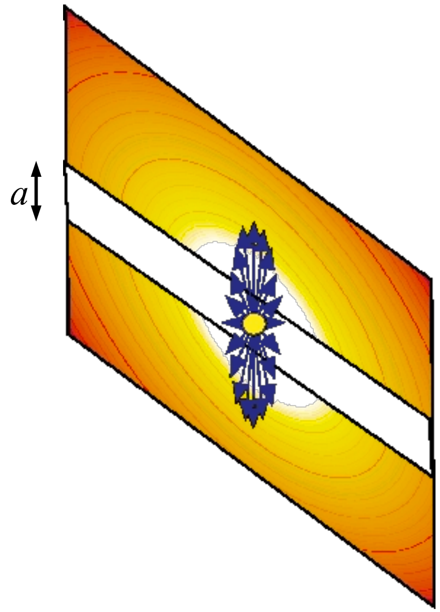

Principle of ODR Diagnostics

- imaging with ODR: no beam image, illuminated slit
  → seems not suitable for beam diagnostics
  nevertheless, attempts to use ODR imaging:
  A. Lumpkin et al., Proc. BIW 2008, TUPTPF061

D. Xiang et al., PRST AB 10, 062801 (2007)

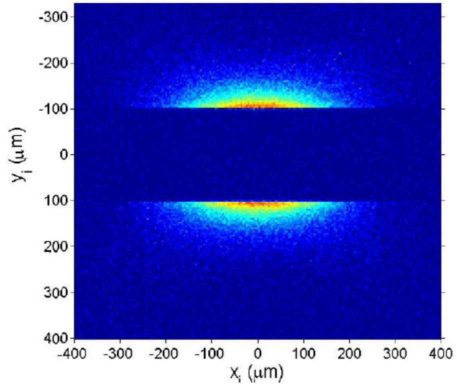

- exploit ODR angular distribution:
  visibility of interference fringes can be used to determine transverse size of a bunch of electrons crossing the slit
  → increasing σ_y both the peak intensity and the central minimum increase

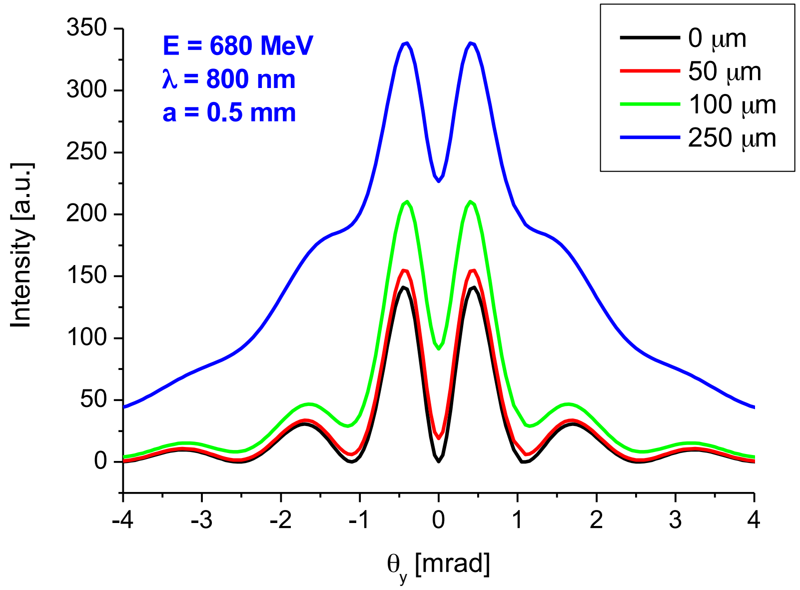

courtesy: E. Chiadroni (INFN)

- research project @ FLASH

ODR Evidence

- CCD image

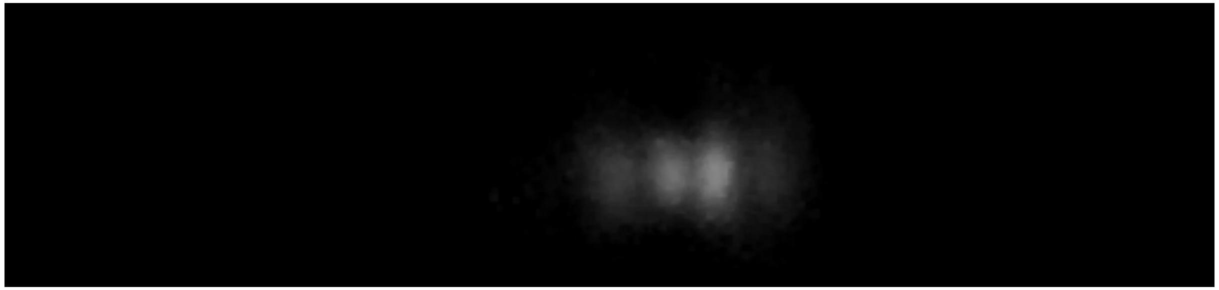

Beam transport optimization
- 0.7 nC
- 25 bunches
- 2 s exposure time
- E_{beam} (nominal) = 680 MeV
- 800 nm filter and polarizer in

- comparison

Simulation parameters:
- a = 0.5 mm
- Gaussian distributed beam
- σ_y = 80 μm
- σ'_y = 125 μrad
- E_{beam} = 610 MeV

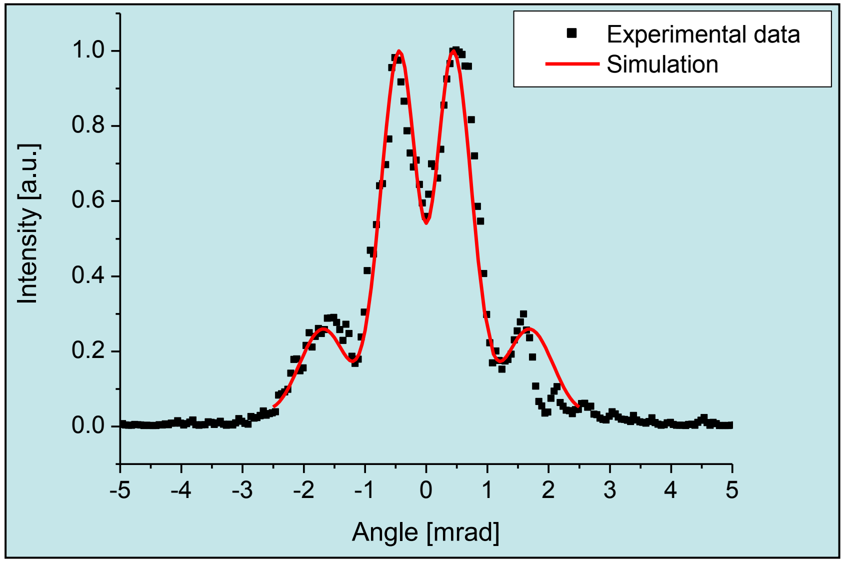

E. Chiadroni, M. Castellano, A. Cianchi, K. Honkavaara, G. Kube, V. Merlo, F. Stella,
Non-intercepting electron beam transverse diagnostics with optical diffraction radiation at the DESY FLASH facility
NIM B 266 (2008) 3789–3796 *and* ***Proc. of PAC 2007, p.3982***

ODR Interferometry (ODRI)

- reduction of synchrotron radiation background

courtesy: E. Chiadroni (INFN)

→ stainless steel shield in front of ODR screen with larger cut

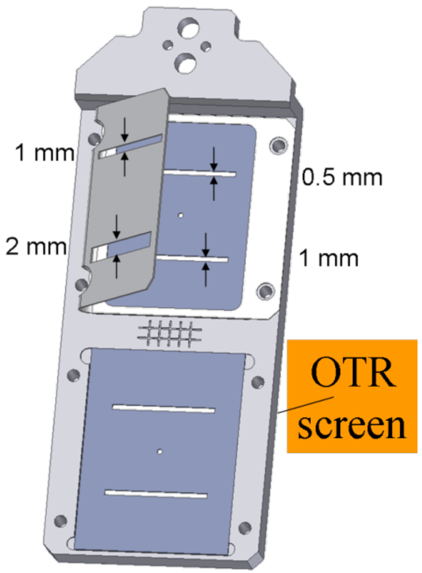

In the case of a wavelength of 800 nm and 1 GeV beam energy the 1 mm cut is not large enough to prevent the production of ODR in the forward direction, reflected by the screen and interfering with the backward ODR produced by the screen itself.

An ODR analogous of the Wartski interferometer used for OTR, with the difference that in this case the two interfering amplitudes are different in intensity and angular distribution

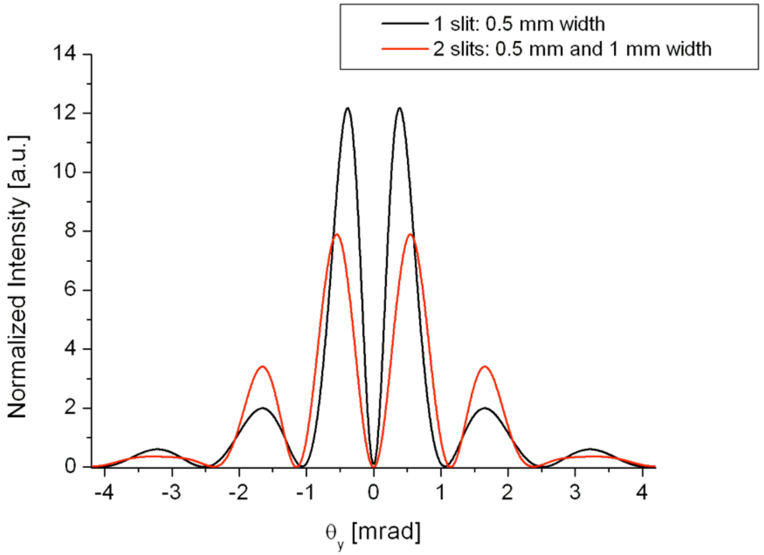

Single particle going through the center of both slits with 900 MeV energy and 800 nm wavelength

ODRI Measurements

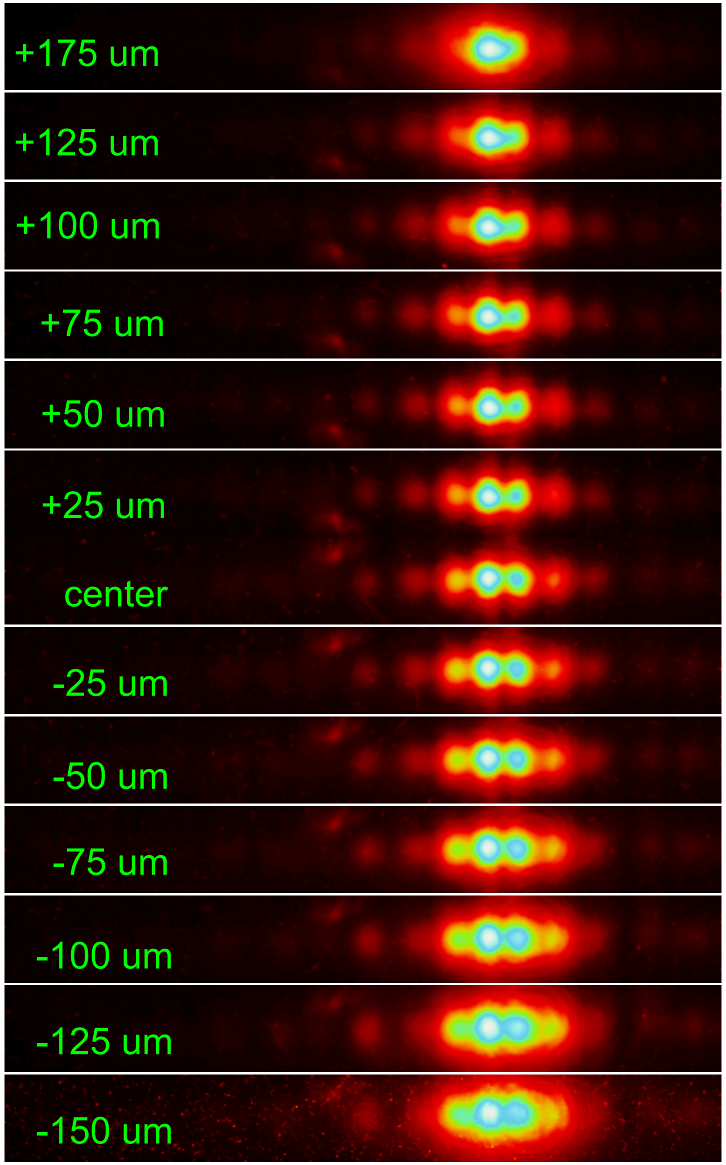

courtesy: E. Chiadroni (INFN)

- transverse scan within the slit
- fit of ODRI angular distribution

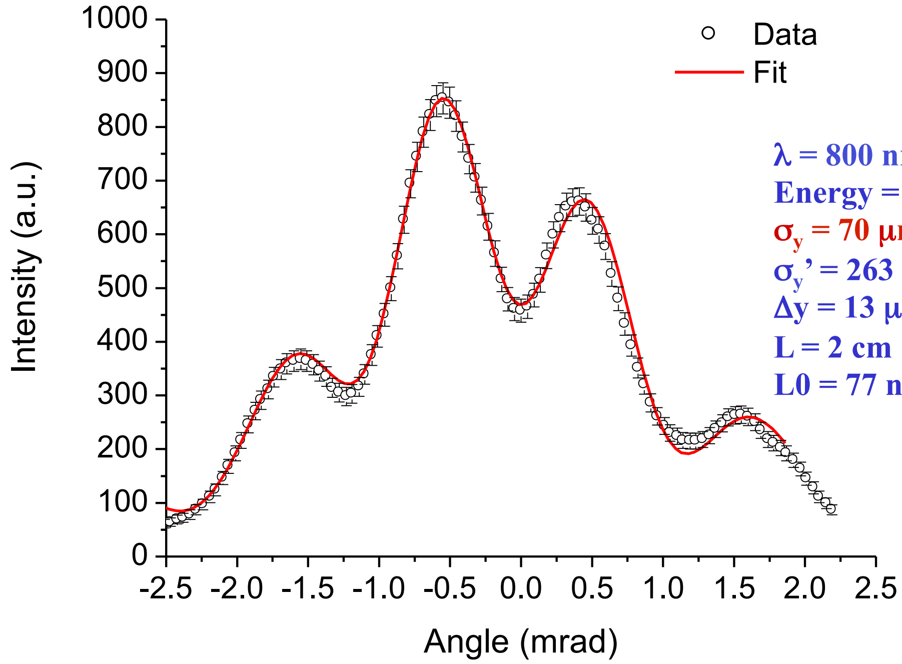

λ = 800 nm
Energy = 865 MeV
σ_y = 70 μm
σ_y' = 263 μrad
Δy = 13 μm
L = 2 cm
L0 = 77 nm

E. Chiadroni, M. Castellano, A. Cianchi, K. Honkavaara, G. Kube,
Optical diffraction radiation interferometry as electron transverse diagnostics
Proc. DIPAC 2009, p.151

⟹ ongoing experiment

OTR/ODR Diagnostics: Pitfalls

- Linac Coherent Light Source (LCLS) @ SLAC

courtesy: H. Loos (SLAC)

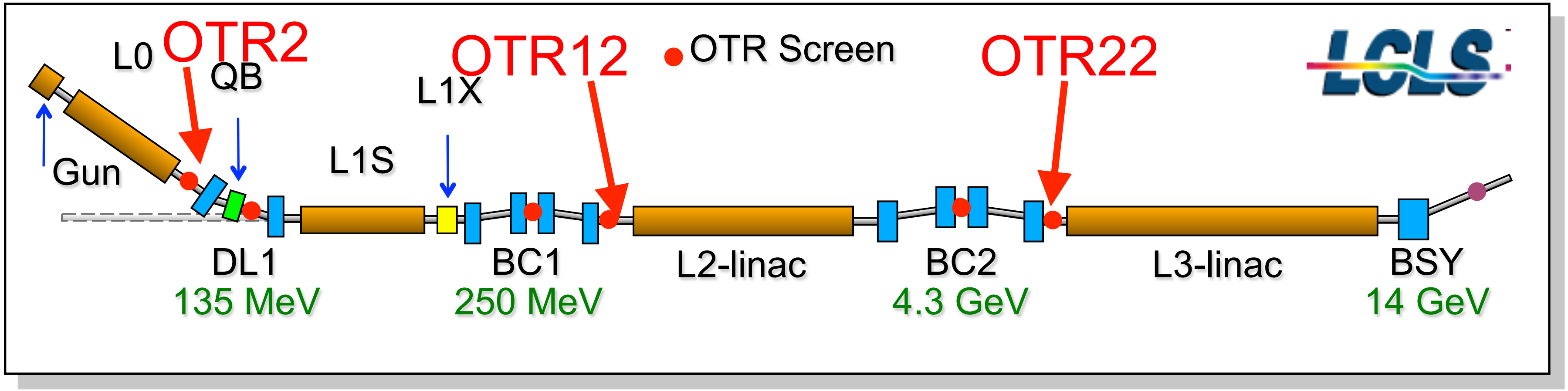

- OTR monitor observation with BC1, BC2 switched on

- OTR 12

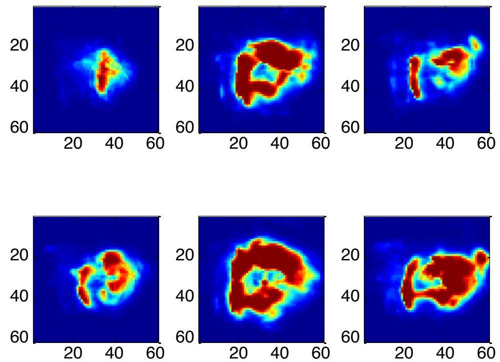

- OTR 22

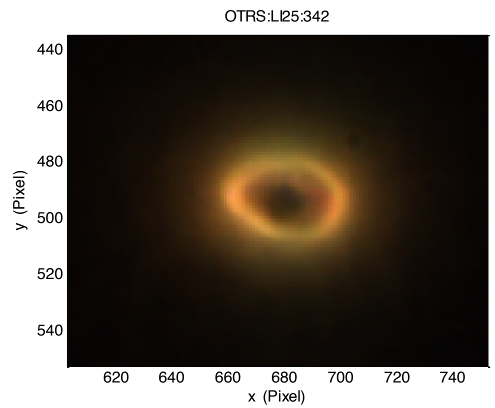

⟹ measured spot is no image of beam

Coherent OTR (COTR)

- interpretation: coherent OTR emission
  - → strong compression in bunch compressors

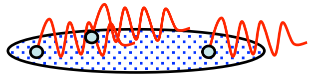

long bunch ($\lambda<\sigma_z$)

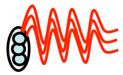

short bunch ($\lambda>\sigma_z$)

- simulation

H. Loos et al., Proc. FEL 2008, p.485

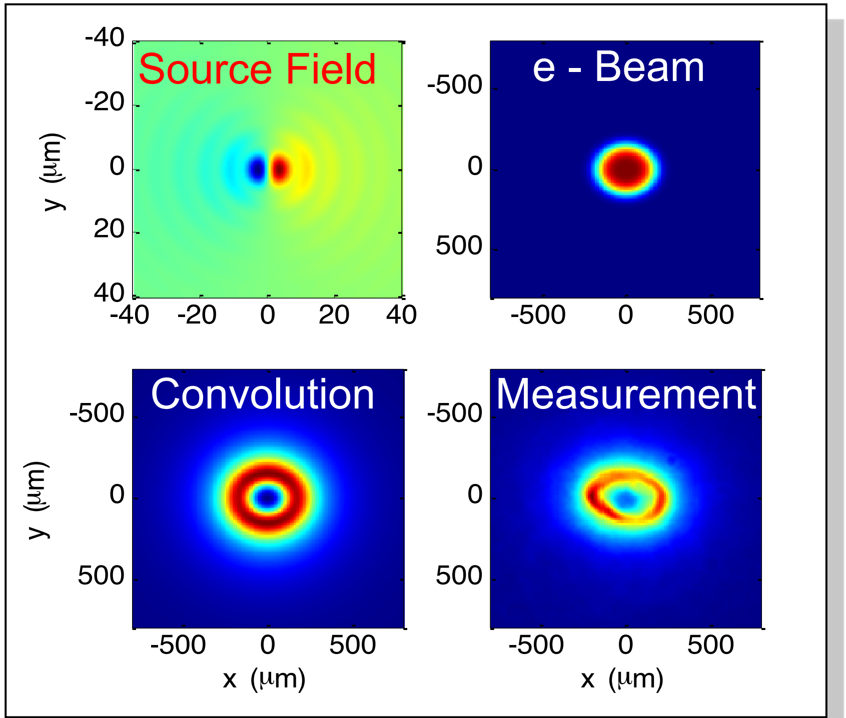

OTR22, 250 pC, 4.3 GeV
10 µm bunch length
100 µm rms beam size
Super-Gaussian

COTR Lineout

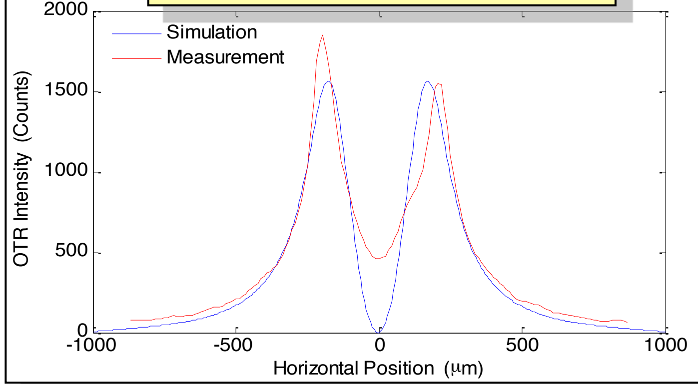

- summary of present knowledge

S. Wesch and B. Schmitt, *Summary of COTR Effects*, Proc. DIPAC'11 Hamburg (Germany), 2011, WEOA01

Consequences

- LCLS: coherent emission compromise use of OTR as reliable beam diagnostics
  - wire scanner for transverse beam diagnostics instead of OTR monitors

- FLASH: COTR observed after modifications to linearize longitudinal phase space

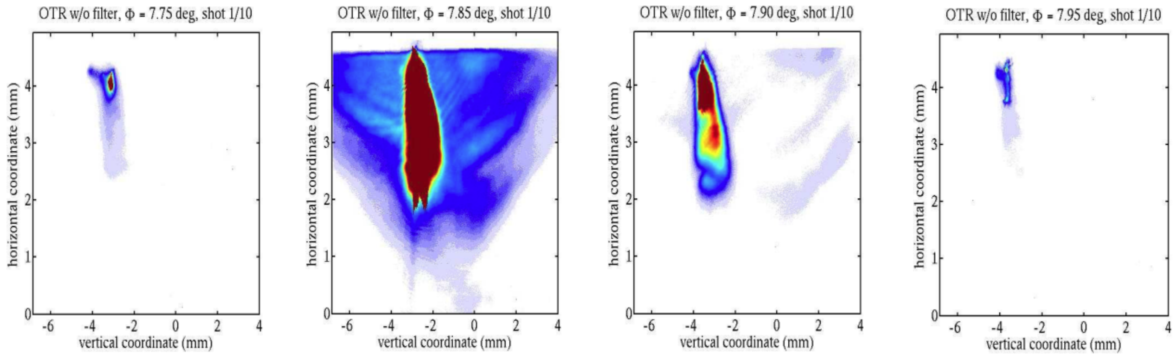

SMATCH screen before FLASH undulator

  - COTR also expected for E-XFEL

- alternative schemes for transverse profile diagnostics
  - TR at smaller wavelengths (EUV-TR): L.G. Sukhikh, G. Kube, Y. Popov et al., Proc. DIPAC‘11 Hamburg, WEOA02
  - screen monitors:

    widely used at hadron accelerators, nearly no information available for high energy electron machines

    B.Walasek-Höhne and G.Kube, *Scintillation Screen Applications in Beam Diagnostics*, Proc. DIPAC‘11 Hamburg, WEOB01

⟹ **ongoing R&D project at DESY**

Inorganic Scintillators

- properties
  - radiation resistant → widely used in high energy physics, astrophysics, dosimetry,…
  - high stopping power → high light yield
  - short decay time → reduced saturation

- generation of scintillation light
  - energy conversion (characterstic time 10^{-18} – 10^{-9} sec)

    Formation of el. magn. shower. Below threshold of e^+e^- pair creation relaxation of primary electrons/holes by generation of secondary ones, phonons, plasmons, and other electronic excitations.
  - thermalization of seconray electrons/holes (10^{-16} – 10^{-12} sec)

    Inelastic processes: cooling down the energy by coupling to the lattice vibration modes until they reach top of valence resp. bottom of conduction band.
  - transfer to luminescent center (10^{-12} – 10^{-8} sec)

    Energy transfer from e-h pairs to luminescent centers.
  - photon emission (> 10^{-10} sec)

    radiative relaxation of excited luminescence centers

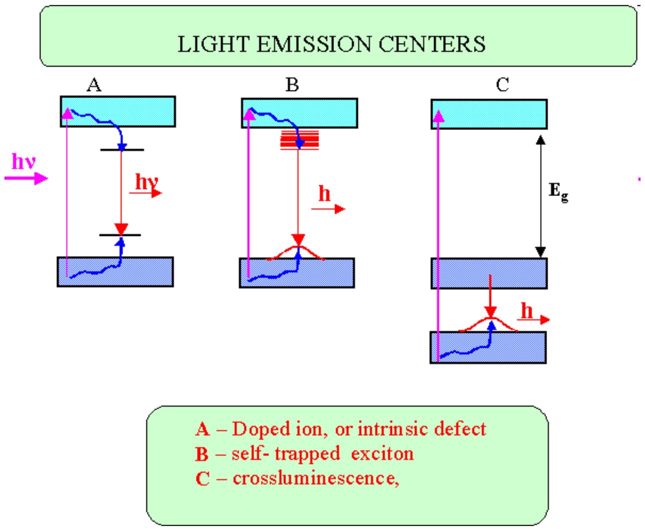

http://crystalclear.web.cern.ch/crystalclear/

Implication on Transverse Resolution

Which effects may affect transverse resolution ?

- light generation: energy conversion → transverse range of ionization
- light propagation → total reflection at scintillator surface

energy conversion

- „thick target“ : formation of electromagnetic shower
  (thickness in the order of radiation length X_0)

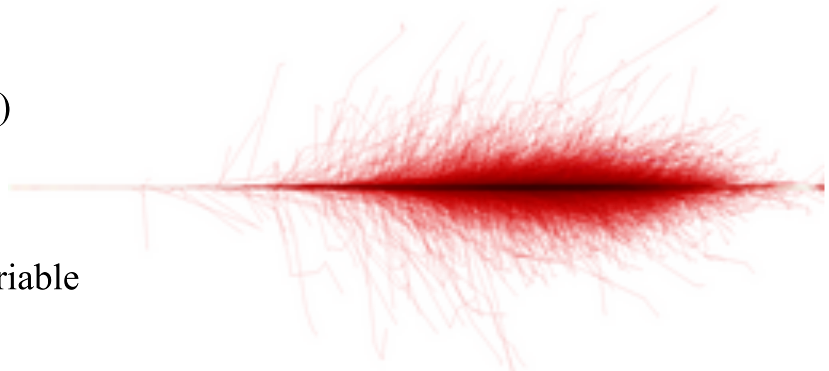

F. Schmidt, "CORSIKA Shower Images", http://www.ast.leeds.ac.uk/~fs/showerimages.html

- transverse shower dimension: ***Molière radius*** as scaling variable
  → containing 90% of shower energy

$$R_M \approx 0.0265\, X_0\,(Z+1.2)$$

X_0: radiation length, Z: atomic number

Implication on Transverse Resolution

- energy loss
  - Bethe-Bloch (collision)
  - Bremsstrahlung (radiative)

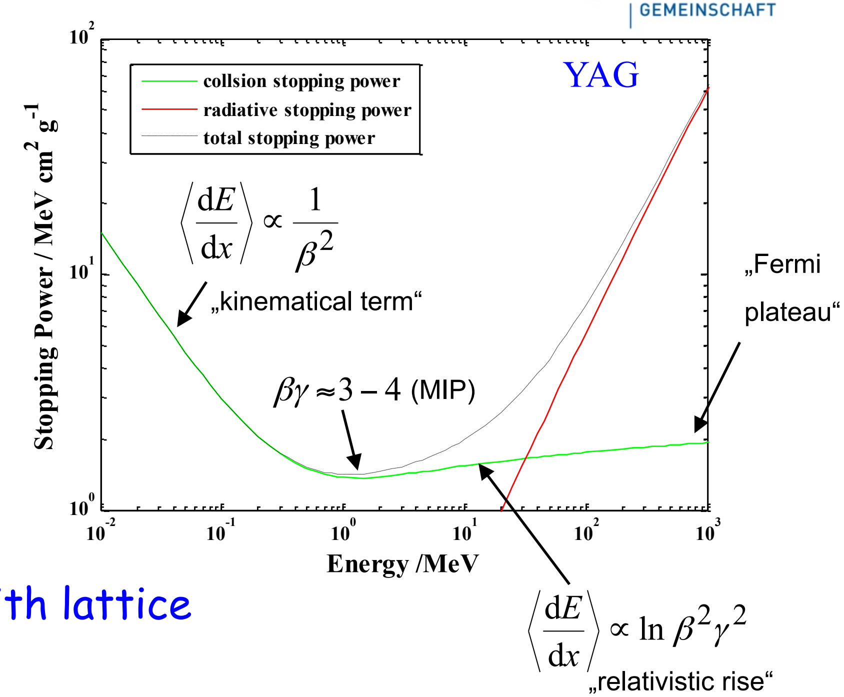

- energy deposition in "thin target"
  - ignore radiative contribution

  - thickness / $X_0 \approx 10^{-2}$

  - small amount of re-absorption in material

- ionization: interaction of particle em. field with lattice
  - particle field

    virtual photons, in classical picture transverse evanescent waves
  - relativistic rise

    incease of transverse field extension
  - Fermi plateau

    cancellation of incoming particle field by induced polarization field of electrons in medium

  → saturation range as scaling variable R_δ

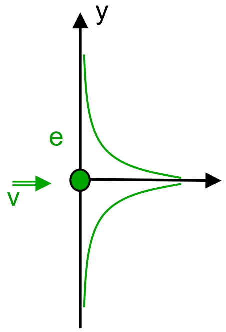

$\vec{E} \propto e^{-y/y_0}$

with $y_0 = \lambda\!\!\!^{-}\, \beta_m \gamma_m$

$\beta_m = \beta\sqrt{\varepsilon(\omega)}$

Implication on Transverse Resolution

- extension radius
  - limiting value:

$$R_\delta = \frac{c}{\omega}\sqrt{1-\varepsilon(\omega)}$$

$\varepsilon(\omega)$: complex dielectric function

  - approximation as free electron gas (Drude model)

$$R_\delta = \frac{\hbar c}{\hbar \omega_p}$$

ω_p: plasma frequency

$$\hbar\omega_p = 28.816\sqrt{\rho\langle Z/A\rangle}\ \text{eV}$$

- light propagation
  - light generated inside scintillator has to cross surface

refractive index n

inorganic scintillators

→ high n, i.e. large contribution of total reflection

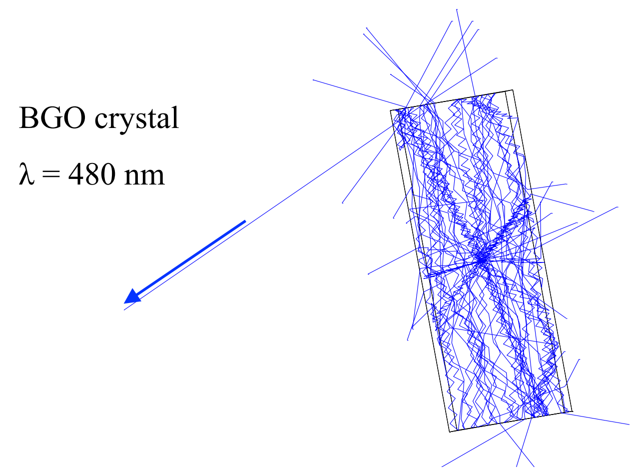

Scintillator Material Properties

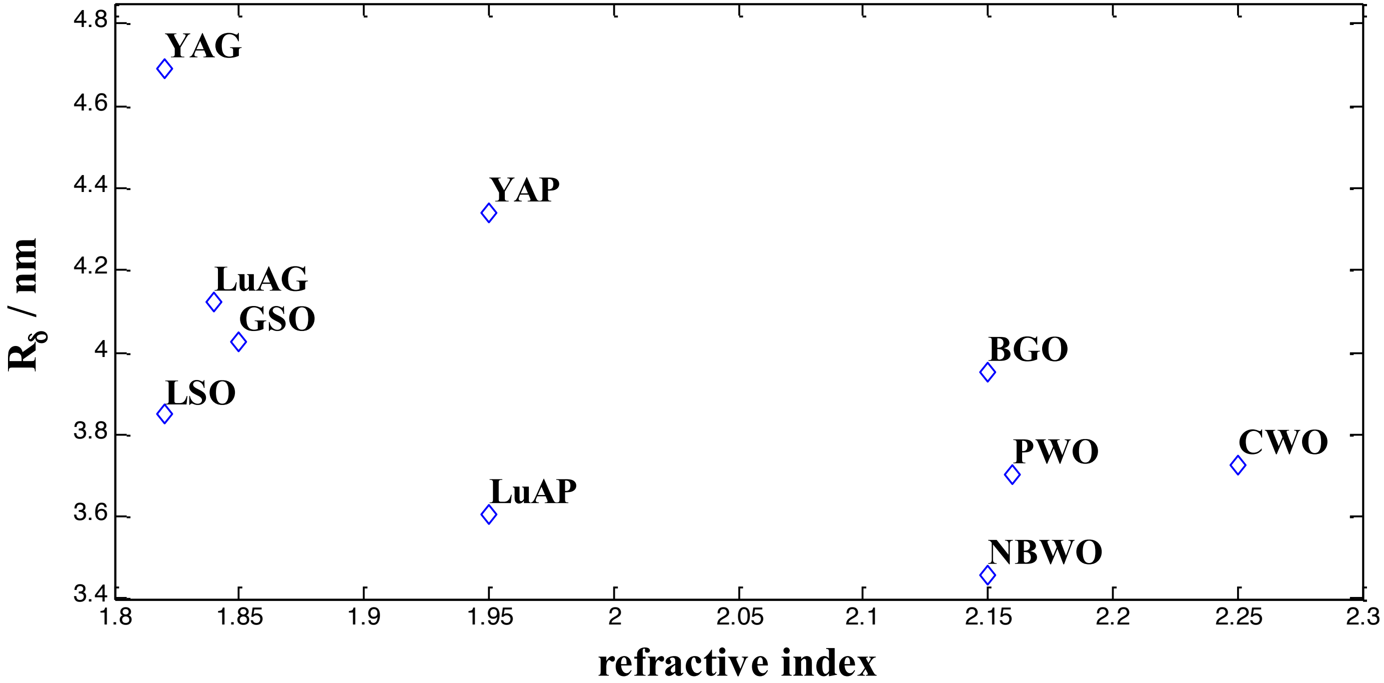

- scintillators under investigation
  - BGO: 0.5 mm
  - PWO: 0.3 mm
  - LYSO: 0.8 mm, 0.5 mm (Prelude 420)
  - YAG: 1.0 mm, 0.2 mm, phosphor

	ρ [g/cm³]	$\hbar\omega_p$ [eV]	R_M [cm]	λ_{max} [nm]	yield [1/keV]	n @ λ_{max}	R_δ [nm]
BGO	7.13	49.9	2.23	480	8	2.15	3.95
PWO	8.28	53.3	2.00	420	0.1	2.16	3.70
LSO:Ce	7.1	51.3	2.08	420	32	1.82	3.85
YAG:Ce	4.55	45.5	2.77	550	11	1.95	4.34

Beam Images

- measurement and analysis: I = 46 pA 5 signal and 1 background frame

› LYSO:Ce (0.5mm)

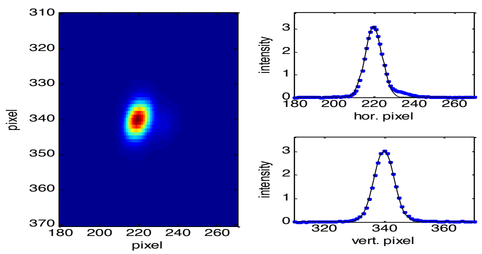

› LYSO:Ce (0.8mm)

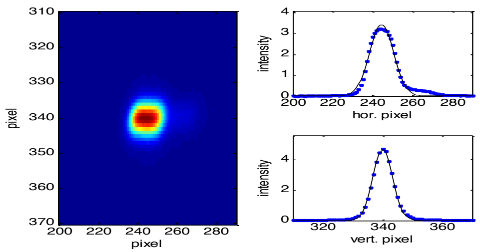

› YAG:Ce (powder)

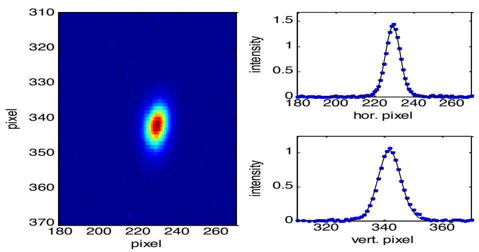

› YAG:Ce (0.2mm)

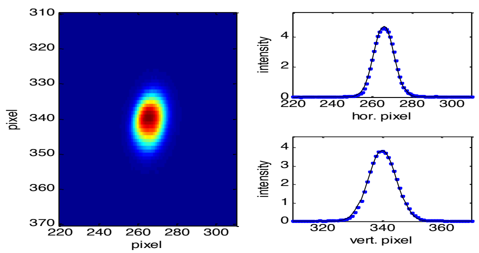

› BGO (0.5mm)

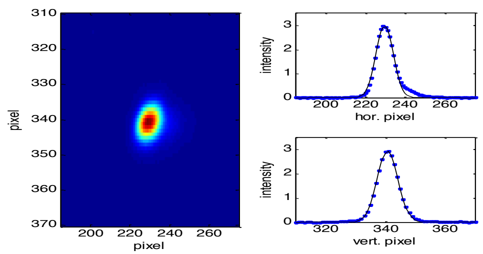

› PWO (0.3mm)

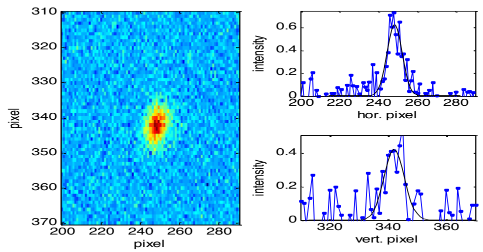

› YAG:Ce (1mm)

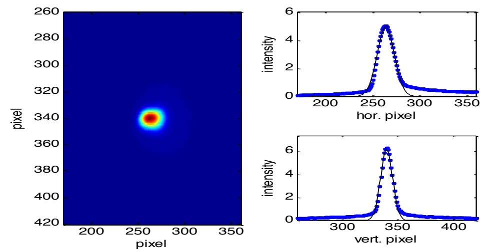

different scale !

› Al_2O_3 (0.5mm)

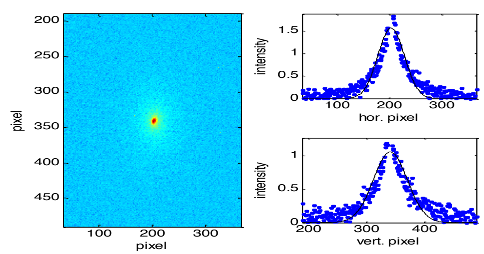

Results

- vertical beam size

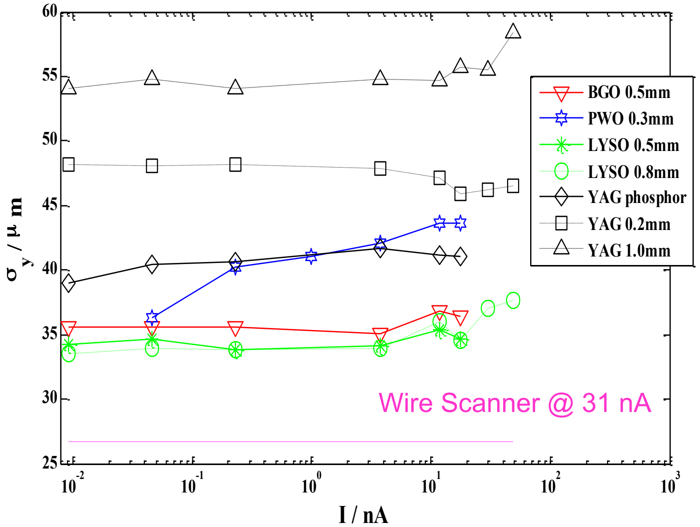

- horizontal beam size

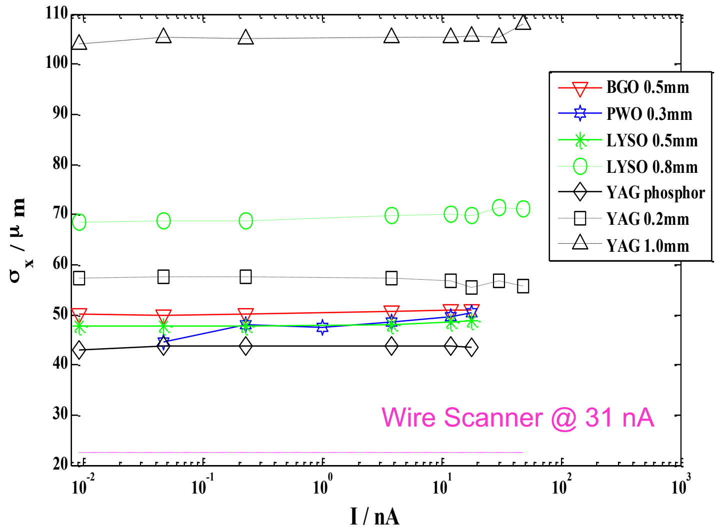

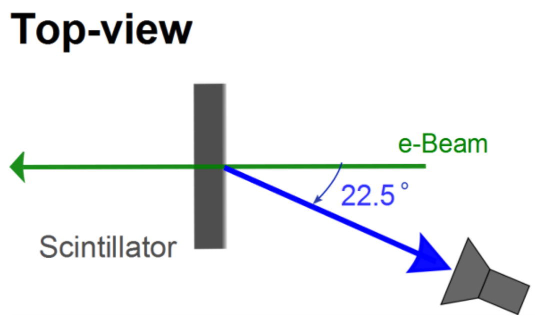

favorites: BGO and LYSO

⟹ dependency on observation geometry

G. Kube et al., Proc. IPAC'10, Kyoto (Japan), 2010, p.906

Results

- results confirmed in additional experiment
  - screen thickness: 0.3 mm

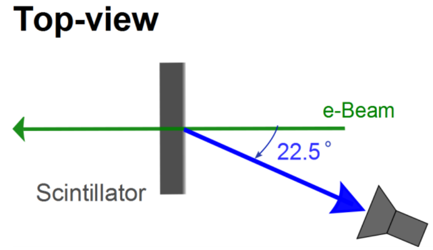

resolution of different materials

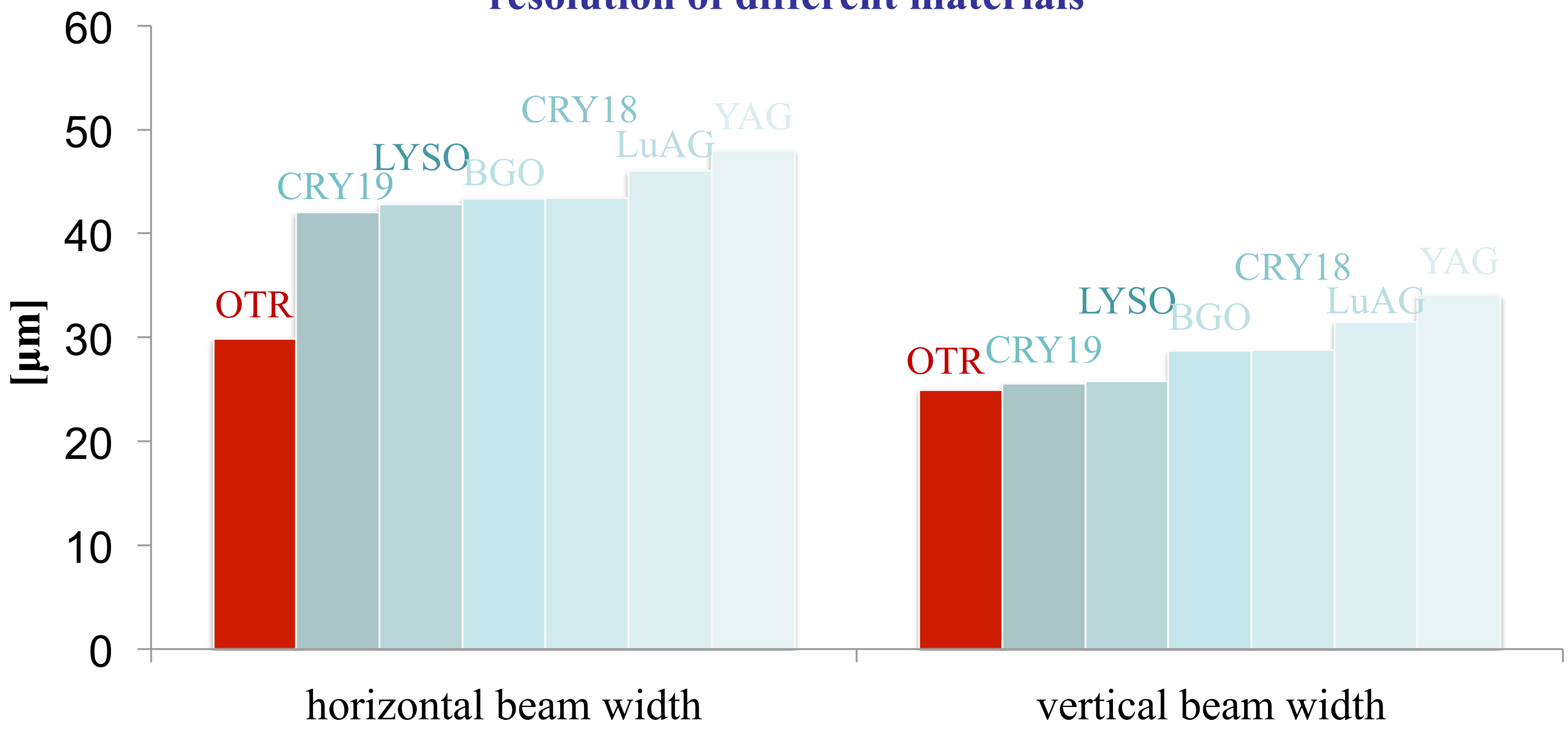

Observation Geometry

- beam diagnostics
  → popular OTR-like observation geometry:

45°tilt of screen

observation under 90°

→ **turns out to be bad!**

- scintillator tilt versus beam axis

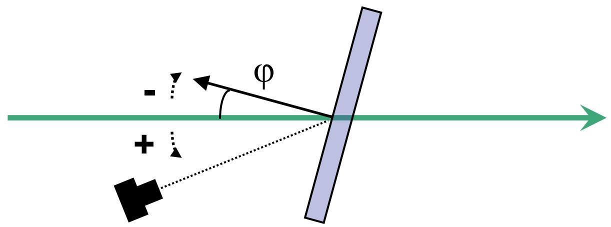

BGO crystal

micro-focused beam

I = 3.8 nA

- measured beam spots

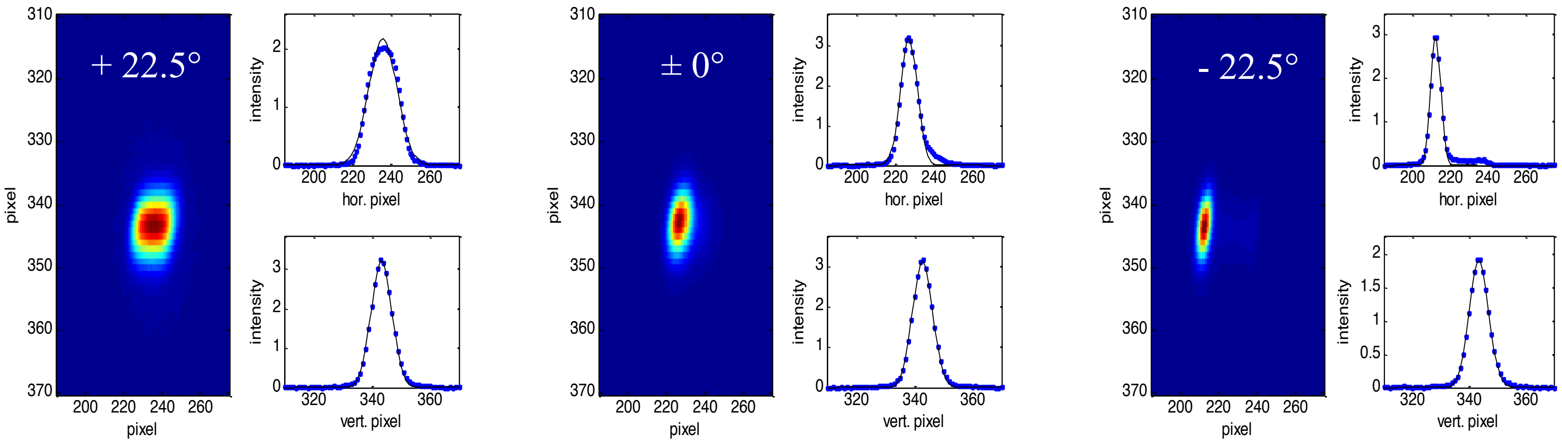

› experimental results confirmed by simulation

G. Kube et al., Proc. IPAC'10, Kyoto (Japan), 2010, p.906

Observation Geometry Influence

- confirmed by new experiment

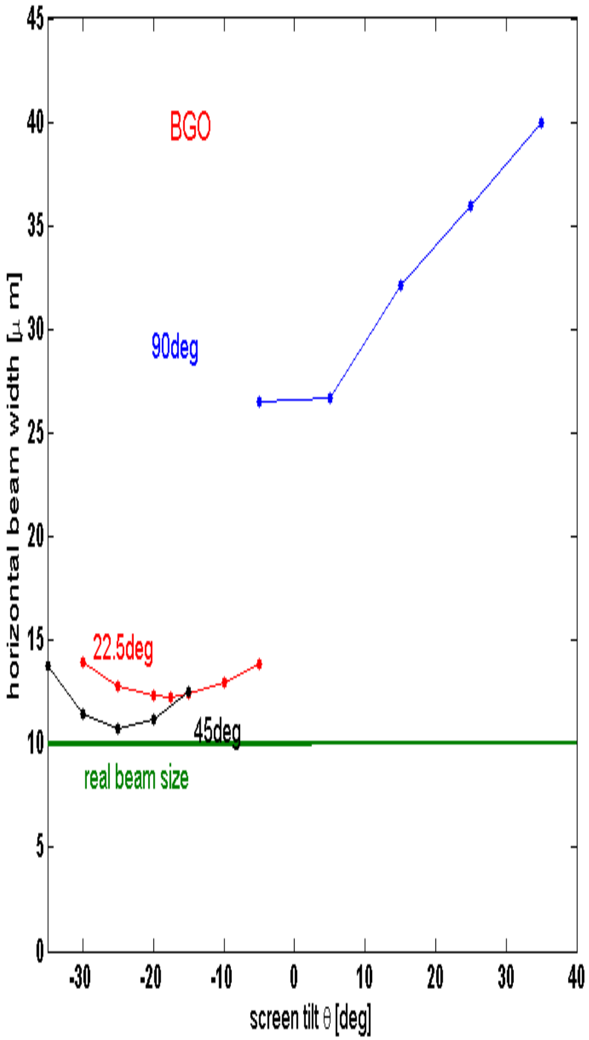

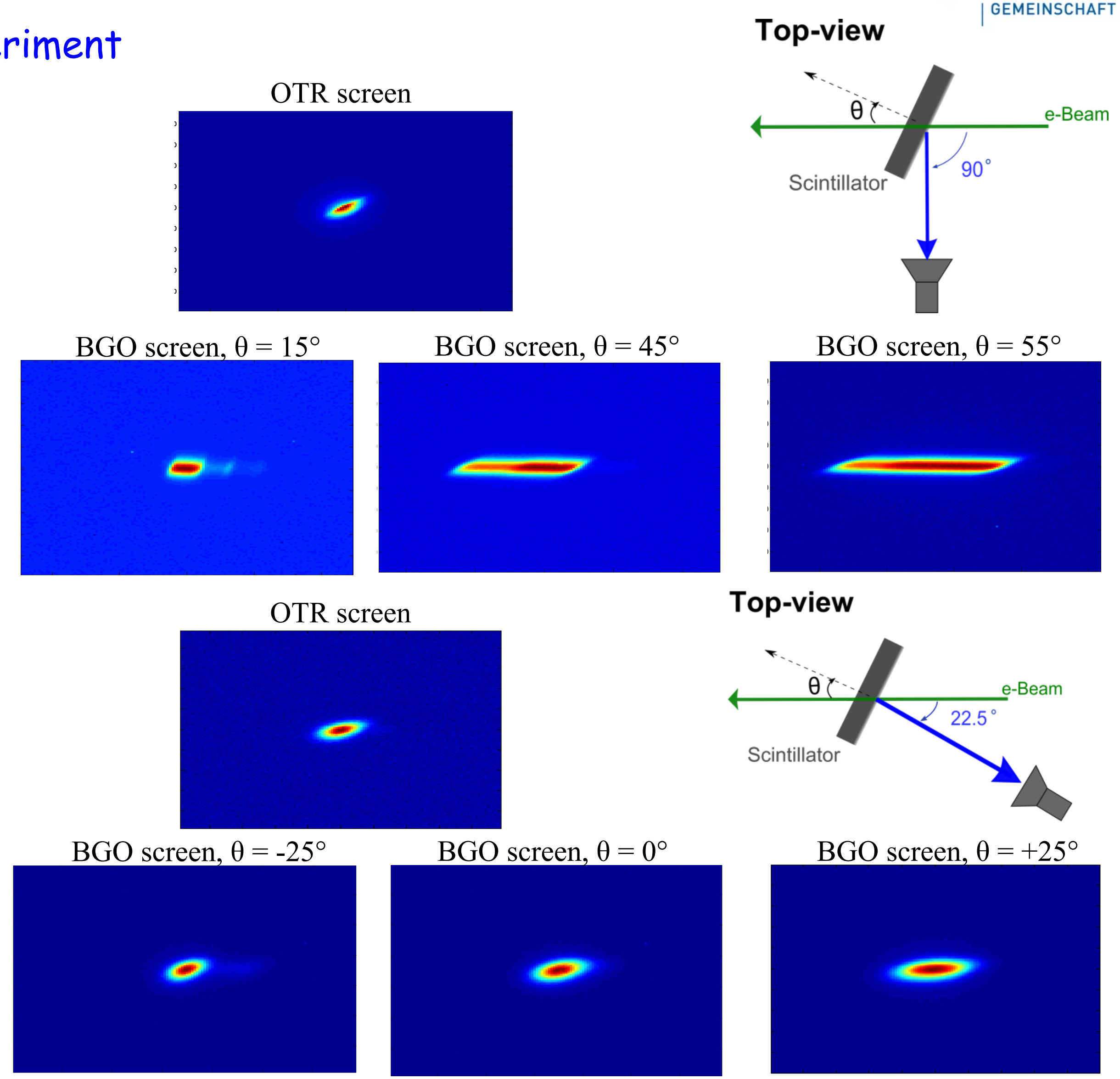

R&D Program on Screens @ DESY

- OTR generation at scintillation screen
  - boundary between scintillation screen and vacuum
    - → (C)OTR generation
    - → may be reflected to detector

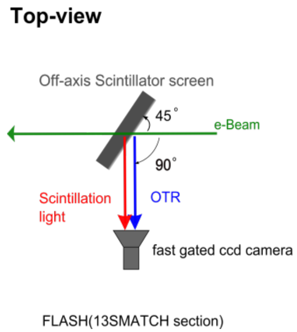

- investigation of temporal suppression of COTR on screen surface
  - **basic idea:** OTR emission is instantaneous process, scintillation light emitted with delay
    - → read-out with gated camera: camera delay ≥ scintillation light decay time

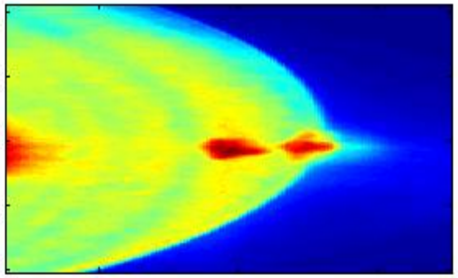

Al coated Si OTR screen:
COTR light,
coherent SR

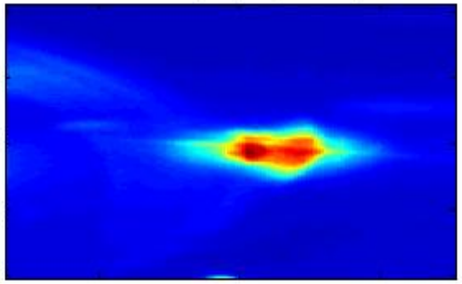

LuAG screen:
COTR & scintillation light

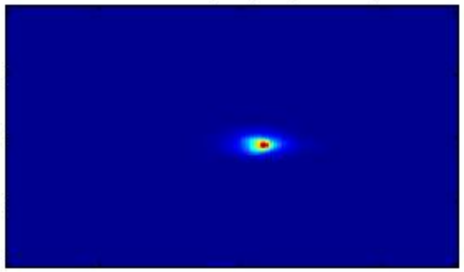

LuAG screen
+100ns delay
only scintillation light

  - first tests successfuly performed
    - → M. Yan et al., Proc. DIPAC'11 Hamburg, TUPD59

- spatial suppression under investiagtion

Storage Rings (Electrons)

- transverse profile / emittance
  - **imaging** with **synchrotron radiation (SR)**
    - → non-destructive profile diagnostics
  - HERA e beam size: s_{hor} = 1200 mm, s_{vert} = 250 mm
    - → resolution with **optical SR** sufficient
  - problem: **heat load** on **extraction mirror** (X-ray part of SR)
    - → material with low absorption coefficient (Be)
    - → cooling of extraction mirror
    - → **not sufficient to prevent image distortion…**
  - solutions:

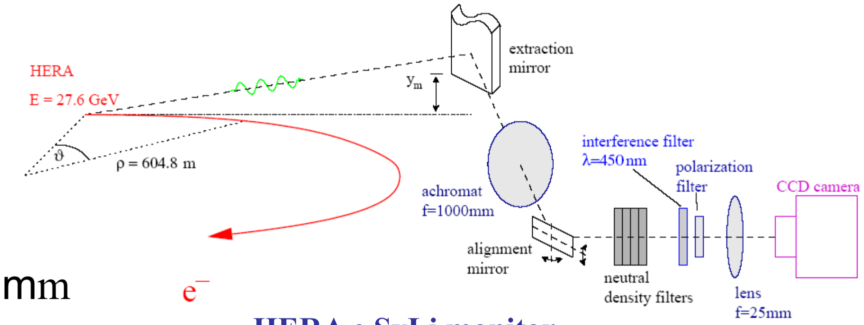

HERA e SyLi monitor

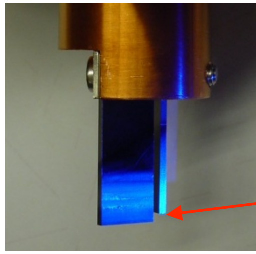

T_{max} = 1200°C

HERA e:

observation out of orbit plane

Photon Factory, LEP: adaptive optics

uncorrected *corrected*

courtesy: T.Mitsuhashi (KEK)

PEP II: slotted mirror

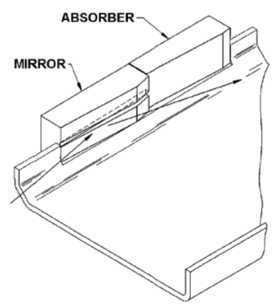

A.S.Fisher et al., Proc. EPAC 1996 , TUP098L

Light Sources: Emittance Diagnostics

- **emittance** typical value **e_x = 1 p nm rad and 1% emittance coupling**
  - principle: synchrotron radiation based diagnostics
  - example: s_{hor} = 40 mm, s_{vert} = 20 mm (PETRA III @ DESY)

SR based imaging: resolution limit (uncertainty principle)

$$\Delta\sigma \approx \frac{\lambda}{2\,\Delta\Psi}$$

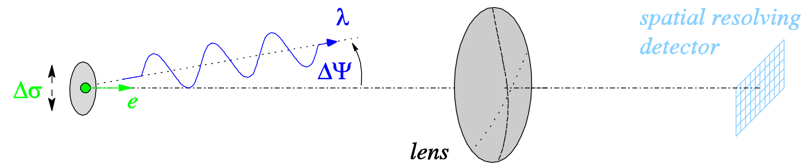

optical imaging: l= 500 nm and DΨ ≈ 1.7 mrad ∩ Ds_{vert}= 150 mm

∩ resolution fully limited by uncertainty principle (diffraction limited)

- widely used schemes for emittance diagnostics

X-ray imaging

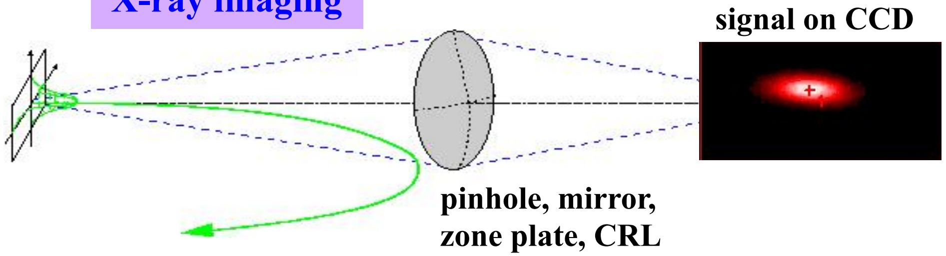

interferometer

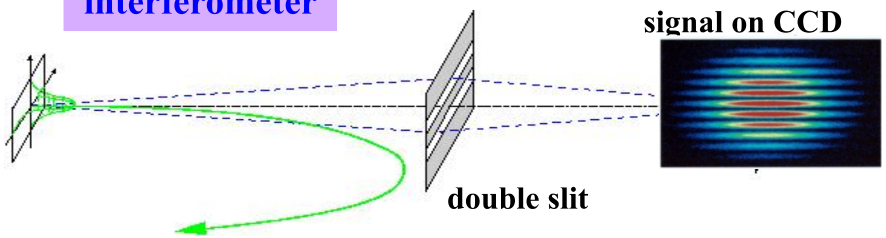

∩ dedicated diagnostics beamline

∩ scanning device, 1 interferometer/plane

Proton Synchrotron Radiation

- SR generated in dipole fringe field

setup :

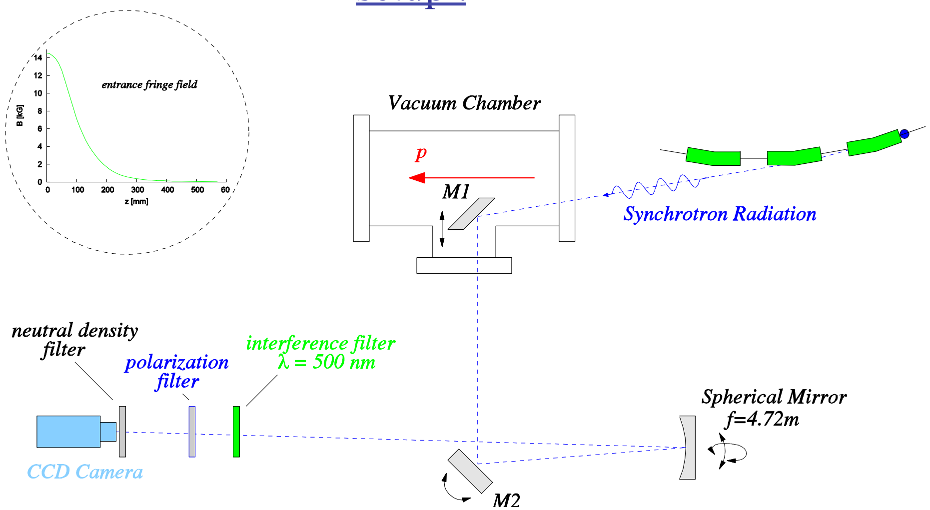

screen shot :

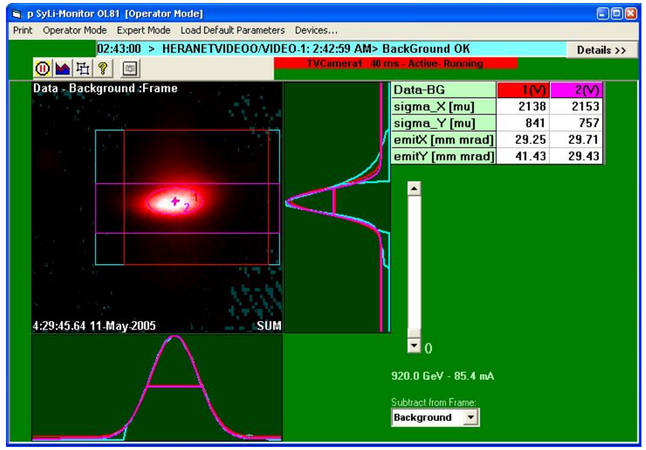

dynamics study:

moving collimators towards the beam

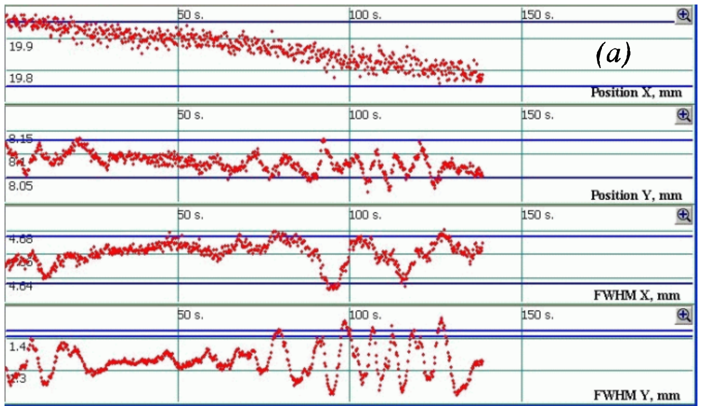

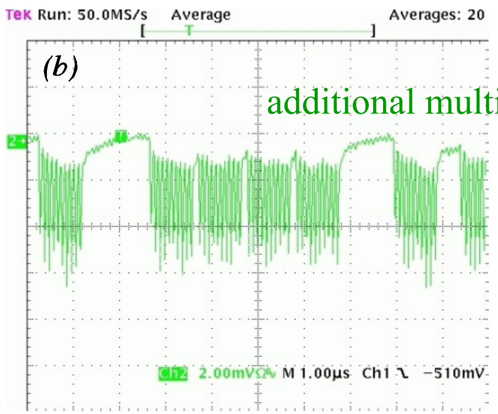

additional multiplier signal

G. Kube et al., Proc. of BIW06 (2006), Batavia, Illinois, p.374

Simulation of Light Propagation

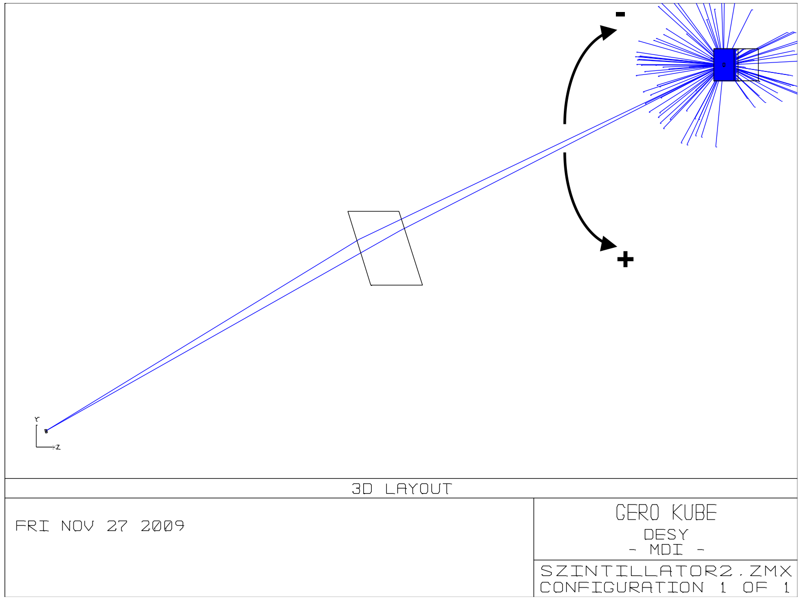

Analysis:

- ZEMAX calculation of 2-dim PSF
- calculation of 2-dim beam profile
- convolution of PSF and beam profile
- horizontal / vertical projection of resulting distribution
- determinatiuon of 2nd moment (standard deviation)

+ 22.5°

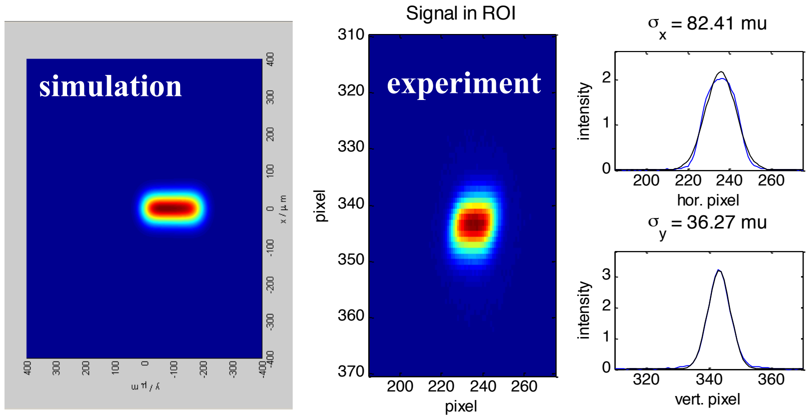

different scale !

0°

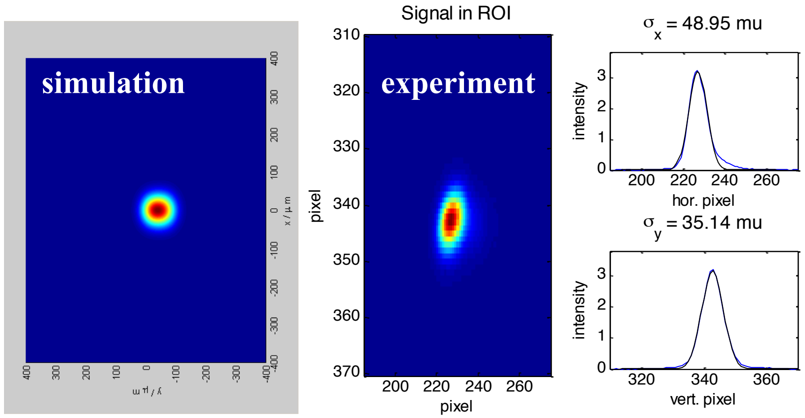

Comparison

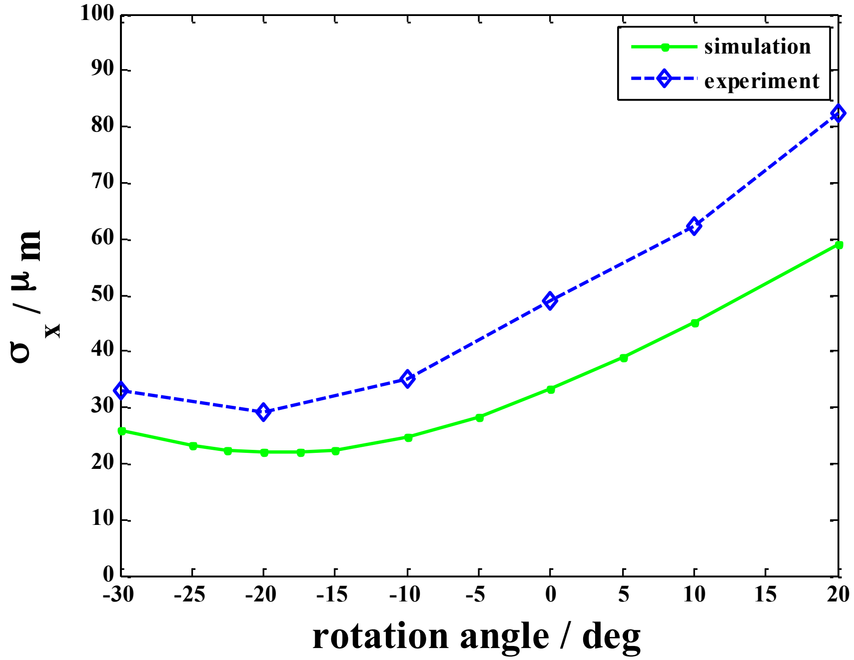

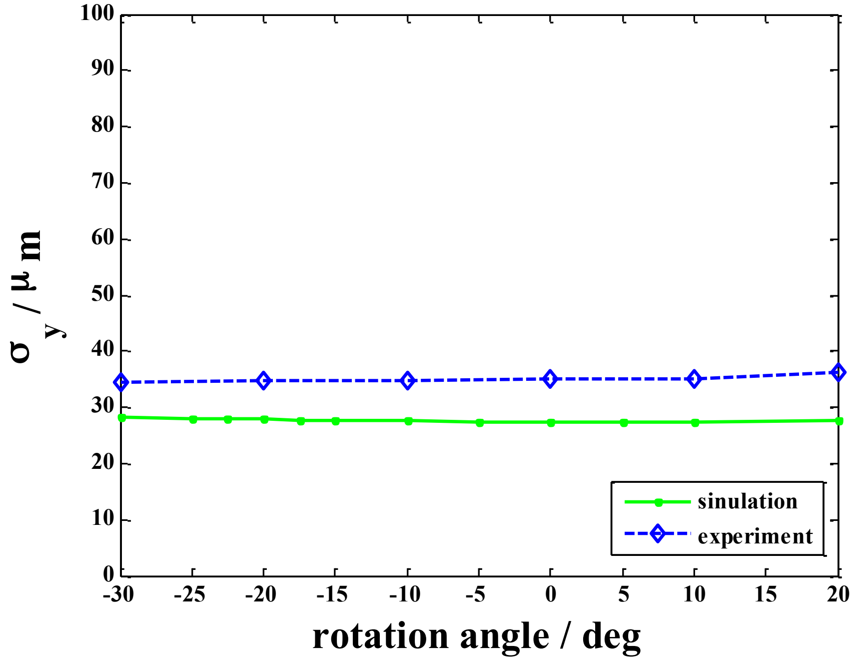

- satisfactory agreement between simulation and measurement

  → simulation reproduces observed trend in beam size

- measured beam size systematically larger than simulated one

  → effect of extension radius not included in calculation → increase in PSF

- results summarized in IPAC'10 proceedings: G. Kube, C. Behrens, W. Lauth, MOPD088

SR Single Particle Time Structure

- geometrical interpretation

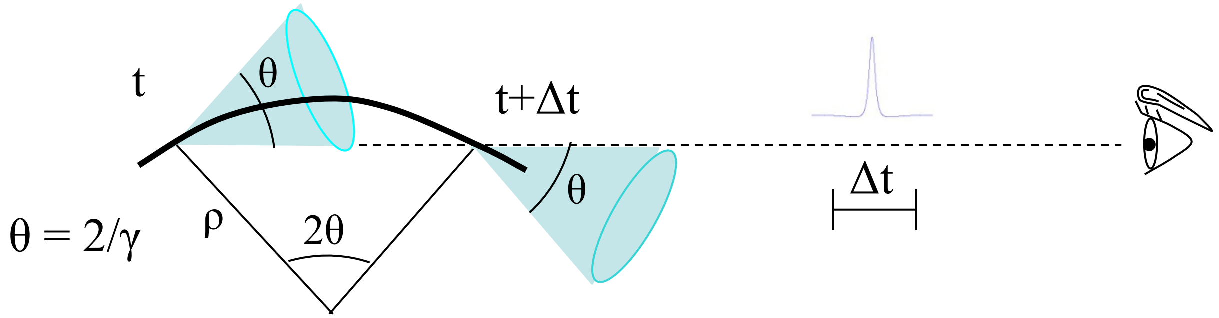

$$\Delta t = \frac{4\rho}{3\gamma^3 c}$$

Δt: distance in travel time between photon and particle

- radiation field in time domain

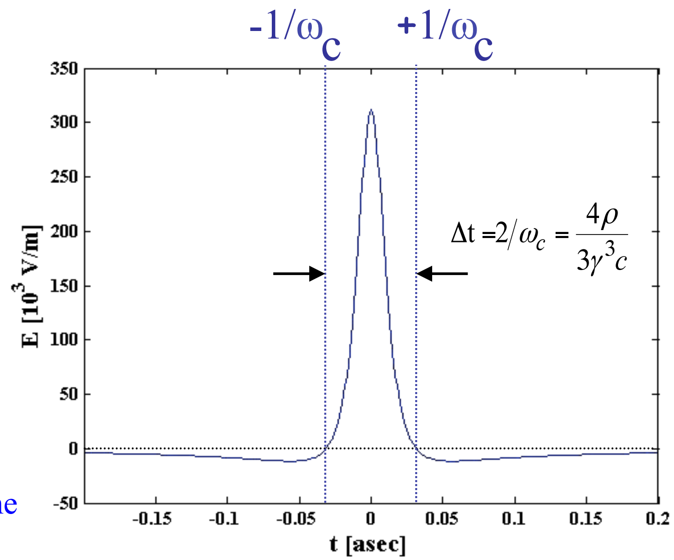

6 GeV electron,

field in orbit plane

consequence:

time interval from maximum to zero crossing defines spectrum (ω_c)

SR Single Particle Time Structure

- comparison

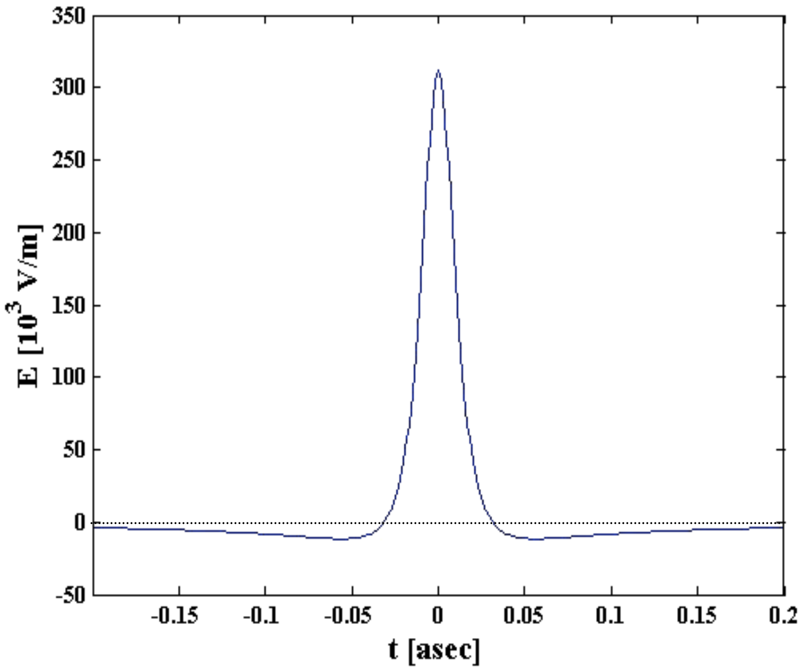

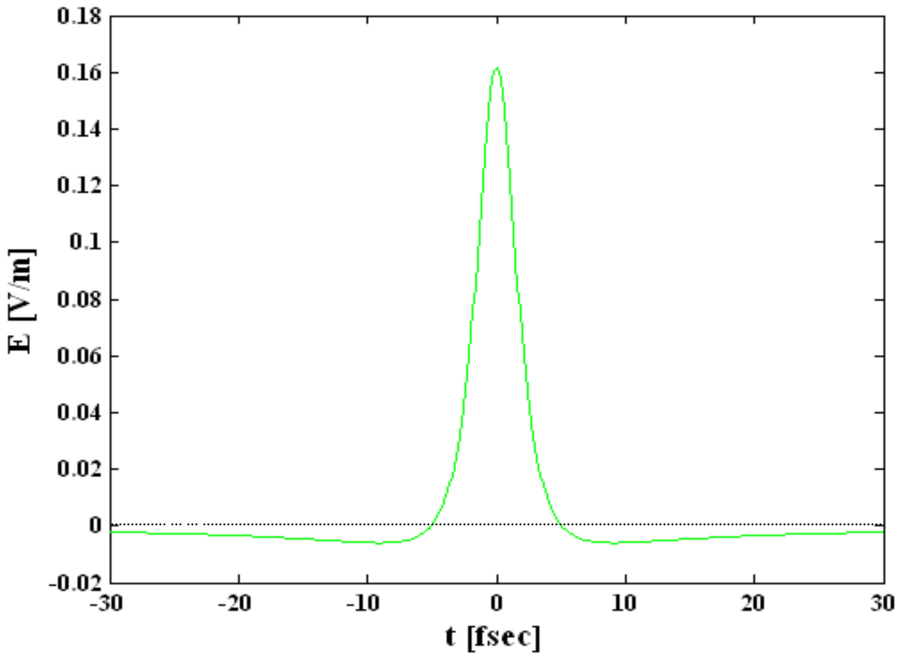

⇒ „squeezing in time" required

SR Single Particle Time Structure

- characteristic time: $$\Delta t_c = \frac{L}{c} \cdot (1-\beta) \approx \frac{L}{2\gamma^2 c}$$ with L: „formation length“

› $L = \frac{2\rho}{\gamma}$ › L: fringe field length › L: magnet length

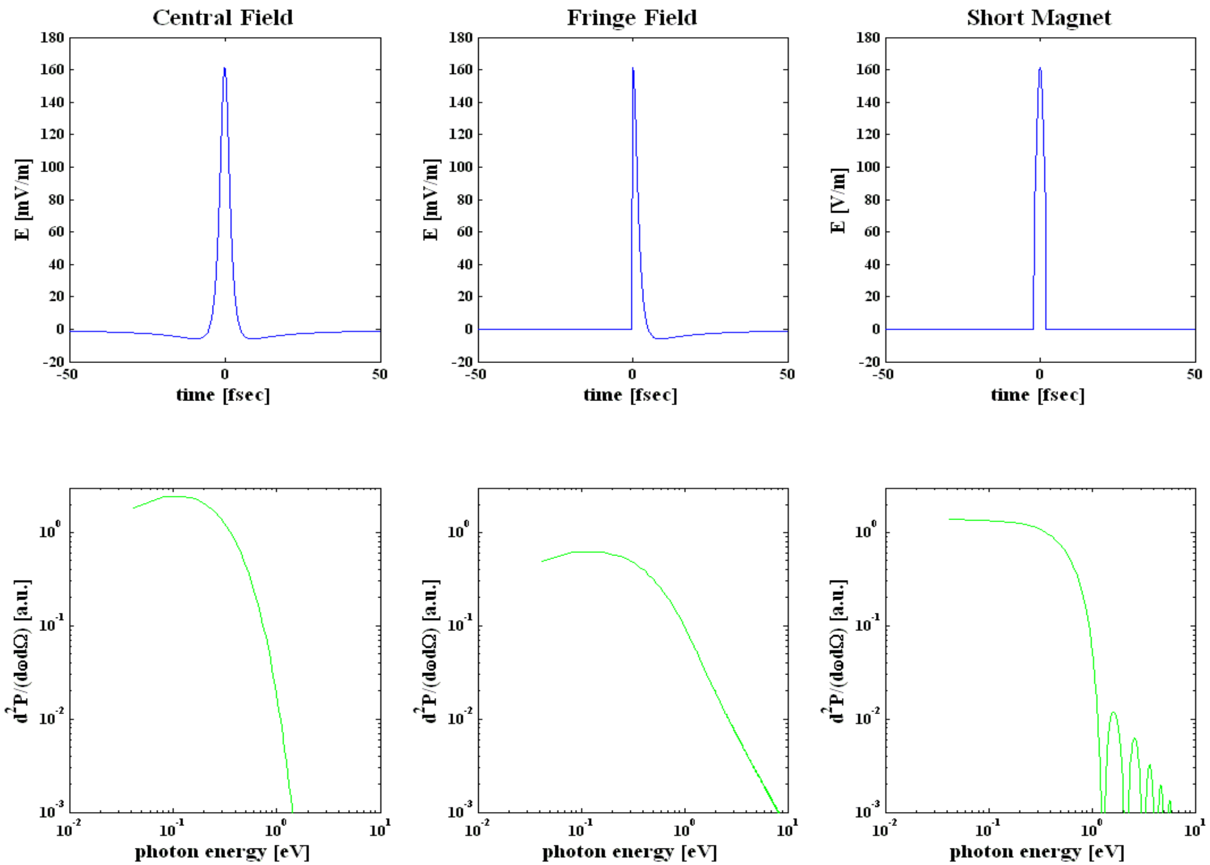

$$\frac{d^2 N}{d\Omega\, d\omega/\omega} \propto \left|\vec{E}_\omega\right|^2$$

with

$$\vec{E}_\omega = \frac{1}{\sqrt{2\pi}} \int_{-\infty}^{+\infty} dt\, \vec{E}(t)\, e^{i\omega t}$$